NASA TM X-789

AL MEMORANDUM

X-789

D TO SPACE VEHICLES IN ORBIT NEAR
CTIONAL INTERPRETATION OF THE
DESIGN AND OPERATIONS DECISIONS

y Charles C. Dalton

Marshall Space Flight Center
untsville, Alabama

AUTICS AND SPACE ADMINISTRATION

December 1962

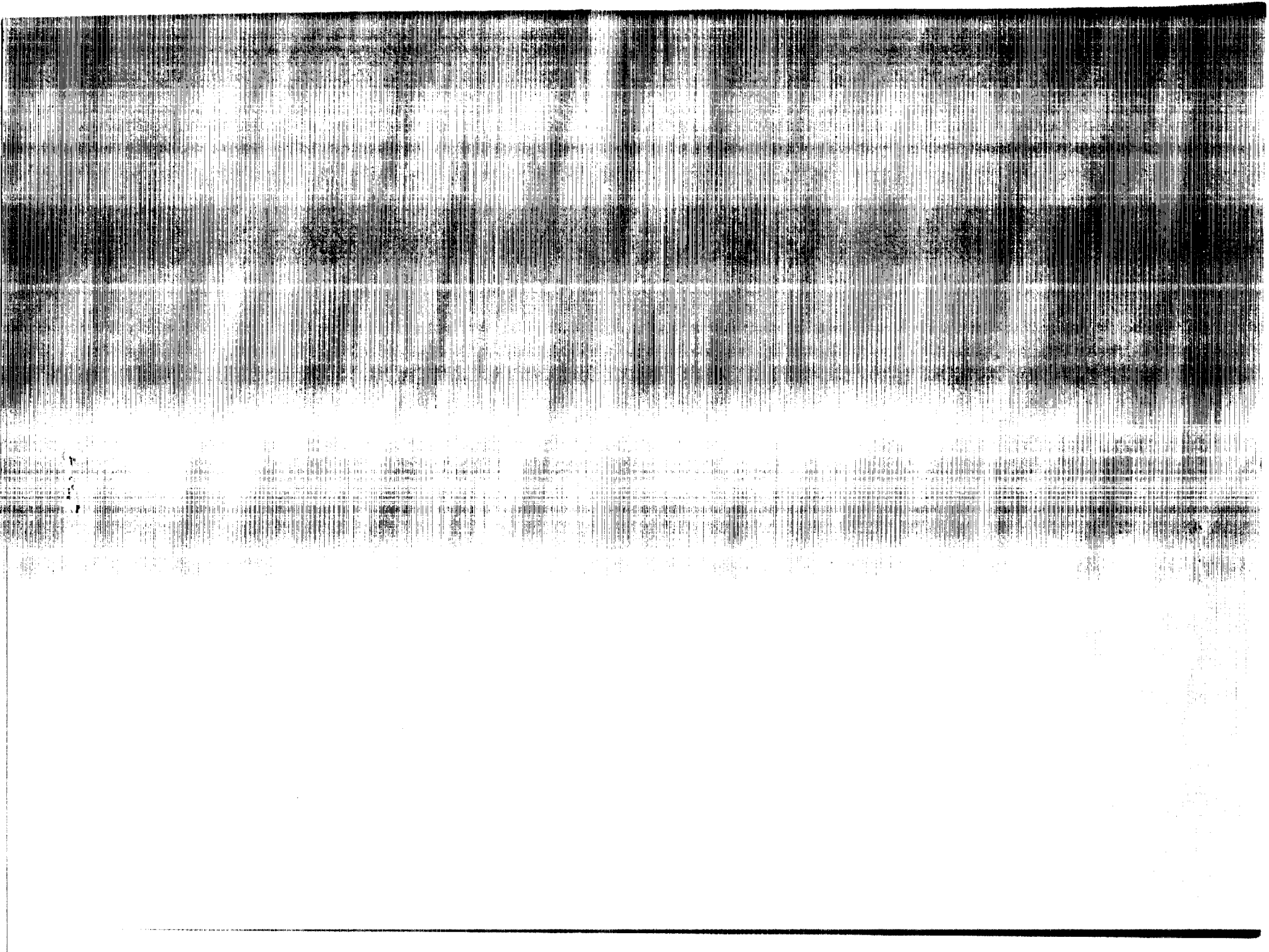

NATIONAL AERONAUTICS AND SPACE ADMINISTRATION

TECHNICAL MEMORANDUM X-789

METEOROID HAZARD TO SPACE VEHICLES IN ORBIT NEAR THE EARTH:* A FUNCTIONAL INTERPRETATION OF THE INFORMATION FOR DESIGN AND OPERATIONS DECISIONS

By

Charles C. Dalton

ABSTRACT

In this survey and analysis of the meteoroid hazard to space vehicles in near-earth orbits,* operations research methods have been used to establish and to propagate confidence levels with respect to all of the pertinent functional relations involving design and operations parameters. The graphically illustrated results show that the wall thickness, necessary for specified operational results, must be increased by a factor 2.00 to increase confidence from 50% to 75%, and that this factor would still be 1.81 if there were no uncertainty with respect to hypervelocity impact phenomena.

Both the median values and the upper and lower fiducial limits for the 50% confidence interval for the mean flux, closing velocity relative to the earth, closing velocity relative to a vehicle in a near-earth orbit, density (specific gravity), just-puncturable thickness of hard aluminum, and just-puncturable thickness of hard stainless steel are shown for values of meteoroid mass between 10 grams and 100 micro-micro grams.

*For this report, near-earth orbits are considered to be of less than 500 km altitude.

Similar limits, the first, second, and third quartiles, are shown for puncture fluxes for walls of hard aluminum and hard stainless steel for thicknesses between 4 centimeters and 4 microns.

Wall-thickness quartiles for 0.85, 0.90, and 0.95 probabilities of no puncture are shown for the hard aluminum and hard stainless steel walls with exposures between 1 square meter second and 1 mega-mega square meter second.

The reader should be aware that there still exists some controversy over the available meteoroid flux, density, velocity, and angular distribution statistics. Therefore, for any design studies the latest accepted values should be employed.

TABLE OF CONTENTS

TABLE OF CONTENTS (CONT.)

LIST OF ILLUSTRATIONS

LIST OF ILLUSTRATIONS (CONT.)

LIST OF SYMBOLS

$x_1, x_2, \ldots$	Any continuous and statistically independent variables
$f(x_1), f(x_2), \ldots$	Probability density functions of x_1, x_2, etc.
$f(x_1, x_2, \ldots)$	Joint probability density function of $x_1, x_2, \ldots$
$\overline{x}_1, E[x_1]$	Average or expected value of x_1
$\sigma_{x_1}, \sigma_{x_2} \ldots$	Standard deviation of $x_1, x_2, \ldots$
$y_i, y_j, \ldots$	Statistically independent normal, i.e., Gaussian, variables
$G, G(x_1, x_2, \ldots)$	Any function of $x_1, x_2, \ldots$ with continuous first partial derivatives
e	Base of natural, i.e., Naperian, logarithms
π	Factor by which circumference exceeds the diameter of a circle
[7] or [e.g., 7]	Reference 7 or for example reference 7
μ	10^{-6} meters
t	Time or duration in seconds, Eq. 154
m(t)	Specific mortality function
km/sec	Kilometers per second
A.U.	Astronomical Unit - earth's radial distance from the sun
gm	Gram
m	Meteoroid mass in grams

LIST OF SYMBOLS (CONT.)

$F_>$	Flux of meteoroids of mass equal to or greater than m; mean number of hits per square meter of surface area of the exposed hemisphere of a spherical vehicle in orbit near the earth, Eq. 37
C	Confidence, defined in Eqs. 18, 22, 27, 28, 29 $0.25 < 0.50 < 0.75$
δ	Proportional increment, defined in Eqs. 18, 22, 26, 27, 29 $-0.6745 \leq \delta \leq 0.6745$
M	Visual magnitude for meteors, Eq. 50
M_u	Highest visual magnitude for which meteoroid velocity is determined
ρ_p	Meteoroid density, i.e., specific gravity, Eq. 95
r_a	Geocentric radial distance to outer edge of earth's atmosphere implicit in meteoroid velocity data
r	Geocentric radial distance to an orbiting spacecraft
v_a	Velocity of a meteoroid at geocentric radial distance r_a relative to the earth's atmosphere, Eq. 56
v_r	Velocity of a meteoroid at geocentric radial distance $r \geq r_a$ relative to the earth's atmosphere
v_∞	Meteoroid hyperbolic velocity excess with respect to the earth
m_e	Mass of the earth
γ	Universal gravitational constant

x_1	Meteor zenith angle, a random statistical value
D_{x_1}	Displacement of the center of the earth from an asymptote of the hyperbolic trajectory of a meteoroid
v_c	Closing velocity between meteoroid and space vehicle in a near-earth orbit, Eq. 62
y_1	An approximately normally distributed random variable showing the uncertainty in the mass dependence of meteoroid flux, Eqs. 37, 44, and 49
β_1	A constant used with y_1, Eq. 48
y_2	An approximately normally distributed random variable showing the uncertainty in the mass dependence of meteoroid velocity relative to the earth's atmosphere, Eqs. 56, 57, and 61
β_2	A constant used with y_2, Eq. 60
y_3	An approximately normally distributed random variable showing the uncertainty in the mass dependence of meteoroid velocity relative to a vehicle in a near-earth orbit, Eqs. 62, 84, and 86
β_3	A constant used with y_3, Eq. 83
y_4, y_5	Approximately normally distributed random variables showing the uncertainty in the mass dependence of meteoroid density, Eqs. 92 through 97, and 99
β_4, β_5	Constants used with y_4 and y_5, Eqs. 92 and 96
p_0	Meteoroid crater depth, Eq. 105, for thick targets

y_6	An approximately normally distributed random variable showing the uncertainty in the velocity dependence of crater depth, Eqs. 100, 102, and 103
β_6	A constant used with y_6, Eq. 101
x_2	The random angle of incidence of a meteoroid relative to the normal to the surface of the vehicle, Eqs. 105 through 108
d	Meteoroid diameter, Eq. 109
ρ_t	Density of the wall material of the space vehicle (target)
H_t	Brinell Hardness of the target material
y_7	An approximately normally distributed random variable indicating the uncertainty in the exponent of the meteoroid penetration coefficient, Eqs. 110 through 113
x_3	The common antilogarithm of y_7, Eqs. 111 and 112
y_8	An approximately normally distributed random variable indicating the uncertainty in the exponent of the density ratio factor, Eqs. 117 through 119
y_{10}	An approximately normally distributed random variable indicating the uncertainty in the exponent of the plate-thickness factor, Eqs. 128 through 132
p	Thickness of a just-puncturable shell under given impact conditions, Eq. 128
x	

ϕ	Puncture flux; the reciprocal of the seconds of mean time between punctures of one square meter of exposed hemispherical surface, Eq. 138
A	Square meters area of the exposed hemisphere of a spherical vehicle, Eq. 164
R	Probability that an exposed area A will not be punctured during time t, Eq. 164

NATIONAL AERONAUTICS AND SPACE ADMINISTRATION

TECHNICAL MEMORANDUM X-789

METEOROID HAZARD TO SPACE VEHICLES IN ORBIT NEAR THE EARTH:* A FUNCTIONAL INTERPRETATION OF THE INFORMATION FOR DESIGN AND OPERATIONS DECISIONS

By

Charles C. Dalton

SUMMARY

When G is a continuous function of the statistically independent chance variables $x_1, \ldots, x_n$, then G is a random variable with the following sufficiently approximate standard deviation:

$$\sigma_G = \left[\left(\frac{\partial G}{\partial x_1}\sigma_{x_1}\right)^2 + \ldots + \left(\frac{\partial G}{\partial x_n}\sigma_{x_n}\right)^2\right]^{\frac{1}{2}} \tag{7}$$

The confidence C in the antilogarithm of an approximately normally distributed chance variable y is the same as the confidence in the variable; i.e.,

$$(C,\ 10^{y}) = (0.25,\ 10^{\overline{y} - 0.6745\sigma_y}),\ (0.50,\ 10^{\overline{y}}),\ (0.75,\ 10^{\overline{y} + 0.6745\sigma_y}). \tag{29}$$

*For this report, near-earth orbits are considered to be of less than 500 km altitude.

For either sporadic or shower meteoroids, impact probability is sufficiently accurately approximated by either a Poisson or a piece-wise-Poisson description with respect to time, depending on whether the available information is specific or general, and on whether one is concerned with specific or average circumstances. But the combined effect for two such hazards also has a Poisson description:

$$R = e^{-A\left[(\phi_{11} + \phi_{12})t_1 + (\phi_{21} + \phi_{22})t_2 + \ldots + (\phi_{n1} + \phi_{n2})t_n\right]}. \tag{34}$$

The number of meteoroids with masses equal to or greater than m grams which should impact per second per square meter of hemispherical exposed area of a vehicle in a near-earth orbit is

$$F_{>} = 10^{y_1} m^{-1.19} \tag{37}$$

where y_1 is an approximately normally distributed chance variable representing the uncertainty in the information and with mean $\overline{y}_1$ and standard deviation σ_{y_1} as follows:

$$\overline{y}_1 = -12.86 \tag{44}$$

$$\sigma_{y_1} = 1.10 \tag{49}$$

This mass dependence of flux is illustrated graphically in Fig. 1.

The velocity in kilometers per second for a meteoroid of mass m grams, just before entering the earth' atmosphere, is

$$v_a = 10^{y_2} m^{0.046} \tag{56}$$

where y_2 is an approximately normally distributed chance variable, which represents both a velocity spectrum and uncertainty in the information about it, with

$$\overline{y}_2 = 1.51 \tag{61}$$

$$\sigma_{y_2} = 0.12 \tag{57}$$

This mass dependence of velocity is illustrated graphically in Fig. 2.

Similarly, the closing velocity with respect to a vehicle in a near-earth orbit is

$$v_c = 10^{y_3} m^{0.041} \tag{62}$$

$$\overline{y}_3 = 1.52 \tag{84}$$

$$\sigma_{y_3} = 0.17 \tag{86}$$

This mass dependence of closing velocity is illustrated graphically in Fig. 3.

The information and the uncertainty about the density or specific gravity ρ to be expected for a meteoroid of mass m grams can be represented by

$$\rho = 10^{0.108 + y_4 + 1.37\, y_5} m^{-1.37} \tag{95}$$

$$\overline{y}_4 = -1.08 \tag{93}$$

$$\overline{y}_5 = -0.079 \tag{97}$$

$$\sigma_{y_4} = 0.073 \tag{94}$$

$$\sigma_{y_5} = 0.075 \tag{99}$$

This mass dependence of density is illustrated graphically in Fig. 4.

A spherical metallic shell (or empty tank) of density ρ_t and of Brinell Hardness Number H_t which, when in a near-earth orbit, must just resist being punctured when hit by a meteoroid of mass m grams, has a necessary wall thickness p centimeters, which is sufficiently accurately represented as having an approximately normally distributed common logarithm with the following mean and standard deviation.

$$E\left[\log_{10} p\right] = 1.06 - 0.29 \log_{10} \rho_t - 0.25 \log_{10} H_t + 0.338 \log_{10} m \tag{134}$$

$$\sigma_{\log_{10} p} = \left\{0.053 + \left[0.204 + 0.056 \log_{10} (\rho_t/H_t) + 0.0046 \log_{10} m\right]^2 + \right.$$
$$+ \left[0.093 + 0.086 \log_{10} \rho_t + 0.0068 \log_{10} m\right]^2 +$$
$$\left. + \left[0.021 + 0.015 \log_{10} m\right]^2\right\}^{\frac{1}{2}} \qquad (135)$$

Two examples of metals which might be used in such manner are:

$$(\rho_t, H_t) = (2.80, 135): \text{ hard aluminum alloy} \qquad (136)$$

$$= (7.42, 310): \text{ hard stainless steel,} \qquad (137)$$

and these are the basis for the results which are illustrated graphically in Figs. 5 and 6.

The number of punctures per second per square meter of exposed hemispherical area of a vehicle in a near-earth orbit can be considered to have an approximately normally distributed common logarithm with mean and standard deviation:

$$E\left[\log_{10} \phi\right] = -9.13 - 3.52 \log_{10} p - 1.01 \log_{10} \rho_t - 0.881 \log_{10} H_t \qquad (139)$$

$$\sigma_{\log_{10} \phi} = \left[1.86 + (0.161 \log_{10} p - 0.0956 + 0.0460 \log_{10} \rho_t + \right.$$
$$+ 0.0401 \log_{10} H_t)^2 + (0.0474 \log_{10} p + 0.666 +$$
$$+ 0.111 \log_{10} \rho_t - 0.0859 \log_{10} H_t)^2 + (-0.0709 \log_{10} p -$$
$$\left. - 0.252 - 0.323 \log_{10} \rho_t - 0.0177 \log_{10} H_t)^2\right]^{\frac{1}{2}}. \qquad (140)$$

These results for the two metals described above are illustrated graphically in Figs. 7 and 8.

The number of centimeters p of equivalent free wall thickness, for a vehicle of hemispherical area A square meters exposed in a near-earth orbit for t seconds, necessary to give a no-puncture probability R, can be considered to have an approximately normally distributed common logarithm with mean and standard deviation given by:

$$E\left[\log_{10} p\right] = 0.284 \left[\log_{10} At - \log_{10} (-\log_e R)\right] - 0.288 \log_{10} \rho_t -$$
$$- 0.25 \log_{10} H_t - 2.37 \qquad (155)$$

$$\sigma_{\log_{10} p} = \left\{0.150 + \left[0.00382\,(\log_{10} At - \log_{10}(-\log_e R)) + \right.\right.$$
$$+ 0.0556 \log_{10}(\rho_t/H_t) + 0.198\Big]^2 +$$
$$+ \Big[0.0057\,(\log_{10} At - \log_{10}(-\log_e R)) + 0.086 \log_{10} \rho_t +$$
$$+ 0.0196\Big]^2 + \Big[0.0129\,(\log_{10} At - \log_{10}(-\log_e R)) -$$
$$\left. - 0.145\Big]^2\right\}^{\frac{1}{2}} \qquad (156)$$

These results are illustrated graphically, in Figs. 9 through 11 for the hard aluminum alloy described in Eq. 136, and in Figs. 12 through 14 for the hard stainless steel described in Eq. 137.

The variance has been resolved into nine independent components, the numerical relative magnitudes of which are presented in Table 1.

Some further sources of uncertainty must be considered in practice, e.g., effects of contents and composite-wall structures.

SECTION I. INTRODUCTION

A. SCOPE

Since about two years ago several excellent reports [e.g., 3, 6, 12, 13, 17, 19, 25, 29, 33, 34, 35, and 41] have been directed specifically toward meteoroid hazards. None of these has dealt with the problem using operations research and systems analysis techniques. These techniques have been effective against similar difficulties in military and other situations [e.g., 7 and 11].

In the five stages described by Way, et.al. [40], in which reports may be most appropriately designated, this report is best described by "In the third stage, review articles appear. These put together data and theories and often come up with a working model, a handy description, ..."

The report is intended to be more than an illustration, and more than a mathematical model. Single-shell-of-metal is the basis of the analysis. Of course, there is considerable interest in composite

bumpers and, e.g., in multiple-sheet structures [e.g., 33]; but it is hoped that the effectiveness of other materials and structures can be considered in terms of the effectiveness of some thickness of single-shell-of-metal. Similarly special considerations must be given for vehicles which: (1) have attitude control or (2) do not remain in a near-earth orbit or (3) do not remain near the ecliptic plane.

B. METHOD

The value that a physical parameter (e.g., length, velocity, etc.) will have under specified circumstances will be uncertain when: (1) the parameter (or the physical process of which the parameter is indicative) may be capricious (e.g., the parameter may be a random statistical variable), (2) the available information may not be either sufficiently firm or direct, or (3) the latter is compounded with the former - as in the present problem - the resulting uncertainty being treated as if it were due to randomness.

ACKNOWLEDGEMENTS

The author wishes to indicate his appreciation for the attentive and constructive efforts of the following persons who reviewed the draft copy of this report:

A. In the Aeroballistics Division, MSFC

Mr. William W. Vaughan
Dr. Ernst D. Geissler
Dr. Willi H. Heybey
Mr. William D. Murphree
Mr. Orvel E. Smith
Mr. Peter Wasko

B. In the Propulsion and Vehicle Engineering Division, MSFC

Dr. John B. Gayle

C. In the Chrysler Corporation

Mrs. Betty Case

D. In the Brown Engineering Company

Mrs. Anita Dietzen
Miss Martha Moorehead

SECTION II. MATHEMATICAL PRINCIPLES

A. FORMAL BASIS

Let $x_1, \ldots, x_n$ be any continuous and statistically independent variables with probability density functions $f(x_1), \ldots, f(x_n)$. Then, because of statistical independence, the joint probability density function can be expressed [e.g., 24] by

$$f(x_1, \ldots, x_n) = f(x_1) \ldots f(x_n) \tag{1}$$

One of the most pertinent of the mathematical statistical concepts is the mean or expected value of a function $g(x_1, \ldots, x_n)$ of the chance variables $x_1, \ldots, x_n$; i.e.,

$$E\left[g(x_1, \ldots, x_n)\right] = \int_{-\infty}^{\infty} \cdots \int_{-\infty}^{\infty} g(x_1, \ldots, x_n) f(x_1, \ldots, x_n) dx_1 \ldots dx_n. \tag{2}$$

By Eqs. 1 and 2, as the $x_1, \ldots, x_n$ are statistically independent,

$$E\left[a_1 x_1 + \ldots + a_n x_n\right] = a_1 E\left[x_1\right] + \ldots + a_n E\left[x_n\right] =$$

$$= a_1 \bar{x}_1 + \ldots + a_n \bar{x}_n \tag{3}$$

and

$$E\left[x_1 \ldots x_n\right] = E\left[x_1\right] \ldots E\left[x_n\right] = \bar{x}_1 \ldots \bar{x}_n \tag{4}$$

where $a_1, \ldots, a_n$ are constants.

A convenient measure of the dispersion of a continuous chance variable x is its standard deviation σ_x, the square root of the second moment with respect to the mean [e.g., 24]; i.e.,

$$\sigma_x = \left[\int_{-\infty}^{\infty} (x - \bar{x})^2 f(x)\, dx\right]^{\frac{1}{2}} \tag{5}$$

By Eqs. 2 and 5, one can define the standard deviation of a random variable x as the square root of the expected value of the square of the

deviation of the variable x from its expected value $\bar{x}$. Therefore, by similarly defining σ_G, the standard deviation of a function $G(x_1, \ldots, x_n)$ of the statistically independent chance variables $x_1, \ldots, x_n$, and using Eqs. 1 and 2

$$\sigma_G = \left[\int_{-\infty}^{\infty} \cdots \int_{-\infty}^{\infty} (G - E[G])^2 \, f(x_1) \ldots f(x_n) dx_1 \ldots dx_n \right]^{\frac{1}{2}}. \tag{6}$$

But Eq. 6 is usually not sufficiently convenient for finding numerical results. The formula, previously argued pragmatically by the author [8], is the same as that which has, for the special case of normal variables, been rigorously derived by Scarborough [36]; i.e.,

$$\sigma_G = \left[\left(\frac{\partial G}{\partial x_1} \sigma_{x_1} \right)^2 + \ldots + \left(\frac{\partial G}{\partial x_n} \sigma_{x_n} \right)^2 \right]^{\frac{1}{2}}. \quad * \tag{7}$$

A more general proof of Eq. 7, for variables not necessarily normal, can be given. When the information about the variables is given by discrete data (e.g., with the values $x_{11}, \ldots, x_{1N}$ for x_1), then for Eqs. 1 and 5,

$$\bar{x}_1 = \frac{1}{N}(x_{11} + \ldots + x_{1N}) \tag{8}$$

$$\sigma_{x_1} = \left\{ \frac{1}{N} \left[(x_{11} - \bar{x}_1)^2 + \ldots + (x_{1N} - \bar{x}_1)^2 \right] \right\}^{\frac{1}{2}}. \tag{9}$$

But by taking the total differential of $G(x_1, \ldots, x_n)$,

$$dG = \frac{\partial G}{\partial x_1} dx_1 + \ldots + \frac{\partial G}{\partial x_n} dx_n \, . \tag{10}$$

Equation 10 is approximately true when all of the differentials are replaced by sufficiently small increments. Assume that the deviations from the mean in Eqs. 8 and 9 are sufficiently small increments.* Then corresponding to the N sets of data for the n variables one has, by substituting into Eq. 10, the N equations

$$G_i - \bar{G} = \frac{\partial G}{\partial x_1}(x_{1i} - \bar{x}_1) + \ldots + \frac{\partial G}{\partial x_n}(x_{ni} - \bar{x}_n) \quad * \tag{11}$$

where $i = 1, \ldots, N$. Therefore, by squaring both sides of Eq. 11, adding the N resulting corresponding equations and dividing by N,

* A more accurate general formula than Eq. 7 would be obtained by including non-linear terms in Eq. 11.

$$\frac{1}{N}\sum_{i=1}^{N}(G_i - \bar{G})^2 = \left(\frac{\partial G}{\partial x_1}\right)^2 \frac{1}{N}\sum_{i=1}^{N}(x_{1i} - \bar{x}_1)^2 + \ldots +$$

$$+ \left(\frac{\partial G}{\partial x_n}\right)^2 \frac{1}{N}\sum_{i=1}^{N}(x_{ni} - \bar{x}_n)^2 + 2\sum_{j=1}^{n-1}\sum_{k=j+1}^{n}\left(\frac{\partial G}{\partial x_j}\right)\left(\frac{\partial G}{\partial x_k}\right)$$

$$\frac{1}{N}\sum_{i=1}^{N}(x_{ji} - \bar{x}_j)(x_{ki} - \bar{x}_k) \qquad (12)$$

where

$$\frac{1}{N}\sum_{i=1}^{N}(x_{ji} - \bar{x}_j)(x_{ki} - \bar{x}_k) =$$

$$= \frac{1}{N}\sum_{i=1}^{N} x_{ji}x_{ki} - \bar{x}_j \frac{1}{N}\sum_{i=1}^{N} x_{ki} - \bar{x}_k \frac{1}{N}\sum_{i=1}^{N} x_{ji} + \frac{1}{N}\sum_{i=1}^{N} \bar{x}_j\bar{x}_k \; . \qquad (13)$$

The last term on the right side of Eq. 13 is identically $\bar{x}_j\bar{x}_k$; and by Eq. 8, the two middle terms are each equal to $-\bar{x}_j\bar{x}_k$; while the first term is the discrete case expression for the expected value of the product of two independent variables x_j and x_k and, therefore by Eq. 4, is also equal to $\bar{x}_j\bar{x}_k$. Therefore, Eq. 13 vanishes and, by Eq. 9, that which is left of Eq. 12, after taking the square root of both sides, is identically Eq. 7.

After the probability density function for a chance variable has been decided, then other interesting results can be derived; e.g., consider a normal variable y with mean $\bar{y}$ and standard deviation σ_y: (1) the probability density function is [e.g., 24]

$$f(y) = (2\pi\sigma_y^2)^{-\frac{1}{2}} e^{-(2\sigma_y^2)^{-1}(y - \bar{y})^2} \qquad (14)$$

(2) there is an even chance that a randomly selected sample of the variable y will have a value within the (probable error) interval

$$\bar{y} - 0.6745\sigma_y \leq y \leq \bar{y} + 0.6745\sigma_y \qquad (15)$$

and (3) the expected value of e^{ay}, where a is a constant, by Eqs. 2 and 14 is

$$E\left[e^{ay}\right] = \int_{-\infty}^{\infty} e^{ay} f(y)\,dy =$$

$$= \int_{-\infty}^{\infty} (2\pi\sigma_y^2)^{-\frac{1}{2}} e^{-(2\sigma_y^2)^{-1}\left[y - (\overline{y} + a\sigma_y^2)\right]^2 + a\overline{y} + \frac{1}{2}a^2\sigma_y^2}\,dy =$$

$$= e^{a\overline{y} + \frac{1}{2}a^2\sigma_y^2}. \tag{16}$$

More generally than by Eq. 15, when x is any continuous random variable, not necessarily normally distributed, with distribution function f(x), then the probability C (confidence) that

$$x \leq x_\delta \tag{17}$$

is related to x_δ and x_L, the lowest possible value of x, by

$$C = \int_{x_L}^{x_\delta} f(x)\,dx \tag{18}$$

where δ is an index by which a particular value of x is established. When x is a differentiable function of a normally distributed random variable y; i.e.,

$$x = x(y) \tag{19}$$

then, symbolically or otherwise, by solving Eq. 19 explicitly for y as a function of x:

$$y = y(x). \tag{20}$$

By applying the technique of Eqs. 2 and 14 to Eq. 19, one can find E[x], the expected value of x, to which there corresponds a value of y by substituting E[x] for x in Eq. 20. Then it should be anticipated that the most appropriate general functional relation between δ and y_δ is

$$y_\delta = y(E[x]) + \delta\sigma_y \tag{21}$$

where: (1) Eq. 15 is a special case, and (2) the x_δ upper limit in

Eqs. 17 and 18 is found by substituting the right side of Eq. 21 for y in Eq. 19. By introductory mathematical statistics [e.g., 24], the f(x) probability density function for x in Eq. 18 is found by: (1) substituting the right side of Eq. 20 for y in the Eq. 14 expression for the f(y) probability density function for y, and (2) multiplying by the absolute value of the derivative of the right side of Eq. 20 with respect to x. Therefore Eq. 18 becomes

$$C = \int_{x_L}^{x(y(E[x]) + \delta\sigma_y)} (2\pi\sigma_y^2)^{-\frac{1}{2}} e^{-(2\sigma_y^2)^{-1}\left[y(x) - \overline{y}\right]^2} \left[\frac{d}{dx} y(x)\right] dx. \tag{22}$$

This Eq. 22 establishes the general functional relation between confidence C and index δ, the Eq. 15 results being only for a special case; i.e., the special case being x = y in Eq. 19.

Another special case with which one necessarily must be concerned here is where, except for a constant coefficient, x in Eq. 19 takes the following functional form:

$$x = e^{\beta y} \tag{23}$$

where β is a constant. Then, by Eqs. 2, 14, and 23,

$$E[x] = e^{\beta\left(\overline{y} + \frac{1}{2}\beta\sigma_y^2\right)} \tag{24}$$

and, by Eqs. 20 and 23,

$$y = (\beta^{-1}) \log_e x. \tag{25}$$

Also, by Eqs. 24 and 25, Eq. 21 becomes:

$$y_\delta = \overline{y} + \tfrac{1}{2}\beta\sigma_y^2 + \delta\sigma_y. \tag{26}$$

Therefore, by Eqs. 21, 23, 25, and 26, Eq. 22 becomes:

$$C = (2\pi\beta^2\sigma_y^2)^{-\frac{1}{2}} \int_0^{e^{\beta\left(\overline{y} + \frac{1}{2}\beta\sigma_y^2 + \delta\sigma_y\right)}} (x)^{-1} e^{-(2\sigma_y^2)^{-1}\left[(\beta)^{-1}\log_e x - \overline{y}\right]^2} dx. \tag{27}$$

So, by Eq. 27, a definite value of C follows from a definite value of δ, the indicated integral having become a definite integral, and x having become a dummy variable - which is related to a more appropriate dummy variable t by:

$$x = e^{\beta(\overline{y} + \sigma_y t)}$$

with which transformation one can write Eq. 27 in the following convenient form:

$$C = \int_{-\infty}^{\delta + \frac{1}{2}\beta\sigma_y} (2\pi)^{-\frac{1}{2}} e^{-\frac{1}{2}t^2} dt \qquad (28)$$

where the values of the indicated integrals are available from tabulations [e.g., 24] of normal areas. But with the tables of normal areas one can show that Eqs. 23, 26, and 28 lead to the following convenient result:

$$(C, 10^{y}) = (0.25, 10^{\overline{y} - 0.6745\sigma_y}), (0.50, 10^{\overline{y}}), (0.75, 10^{\overline{y} + 0.6745\sigma_y}). \qquad (29)$$

B. OPERATIONAL METHODS

What has been done in an uncertain situation? Considerable information (more or less accurate and more or less pertinent) has been painstakingly obtained over many years and at great expense; but it is not amenable to easy and certain application to the meteoroid hazard problem. Some say there is probably a considerable hazard ahead; while others say possible but not very likely. A design decision is upcoming. If the hazard is real, then plans for counteracting it must be made promptly. But if the hazard is illusory, then counteractions will have been an unnecessary bother and expense.

Efforts to gain the much needed new information are being appropriately encouraged; e.g., Whipple [42] is said to indicate that 80% of the needed meteor information may be obtained by terrestrial observation. The results of such efforts will facilitate and improve design decisions which eventually must be made for later spacecraft; but the results will not be available for the present purpose. Reviewing, calculating, and discussing are the only efforts for which there is yet sufficient time; and as a by-product of these efforts one desires also to

learn how most efficiently to expend the forthcoming information-collecting efforts.

In other words, the meteoroid hazard to space vehicles is a typical example of the problems for which operations research methods have been developed. Of course, Ehricke [19] "The [meteoroid flux] numbers, therefore, vary by several orders of magnitude. On this basis, a reliable estimate regarding collision probabilities and erosion effects is obviously impossible" and Rodriguez [35] "The most certain aspect of the hazard to space vehicles from meteoroids is the great uncertainty underlying any attempt at a quantitative assessment of the problem" are right, but more pertinent is Singer's [38] comment "It is generally conceded that measurements of meteoric particles are among the most difficult and uncertain of satellite experiments. But this makes it all the more incumbent on the investigators to report their findings in the greatest detail possible".

C. PROCEDURAL CONVENIENCE

One is justified in going ahead and trying to use to some advantage whatever information can be found regardless of how meager. For example, the following formula derived in [10] relates confidence C that reliability is not less than R when n_t tests have given n_f failures when n_f is a very small but not necessarily vanishing part of n_t:

$$R = \left[e^{-n_f} (1 - C) \right]^{(n_t - \frac{1}{2}n_f)^{-1}} \tag{30}$$

where $0 \leq C \leq 1$ when $n_f = 0$, and where $\frac{1}{2} \leq C \leq 1$ when $n_f \neq 0$. Surely with no failures from two tests it is helpful to think that, based only on demonstrated performance, there is an even chance that the reliability is in the interval $0.50 \leq R \leq 0.87$; or in some other interval determined by hypothetically increasing n_t in Eq. 30 [e.g., 11] to make allowance for information other than test performance. More specifically, what this has to do with procedural convenience is that Poisson statistics were assumed in the derivation of Eq. 30; whereas it is not necessarily strictly true that the failure process in the above example is Poisson. But it was tacitly assumed as a reasonable approximation.

So a procedural convenience is an approximation which is made as an appropriate expedient, without which the analysis would be unacceptably difficult or even impossible. Other examples which could have been

given for illustration are, e.g.: (1) assuming variables to be normal when in fact they may be only very nearly normal, (2) assuming chance variables to be statistically independent when in fact they may have some small correlation, and (3) assuming a curve to be piece-wise constant by representing it by a histogram. But as Davison and Winslow [13] have stated "The common assumption[in space vehicle hazard considerations]is that Poisson statistics describe the[meteoroid] population", and with appropriate reservations," ... the assumption of Poisson statistics as descriptive of the population is not completely unreasonable."

There appears to be some further need for interpreting the use of Poisson statistics as mentioned in several of the reference reports [1-42]. Consider an event which must happen some time and which can happen any time. Then, as Toralballa [39] has shown, the probability density distribution for the occurrence of the event is

$$f(t) = m(t)\, e^{-\int_0^t m(t)\, dt} \tag{31}$$

where m(t) is a function of time which in life statistics is called "specific mortality" and in engineering statistics is sometimes called "failure-rate-of-survivors". Then the product m(t) dt is the conditional probability that if the event has not already occurred by time t then it will occur in the interval between t and t + dt. Then, by the author's derivation shown in a previous report [9], the probability that the event will not have occurred by time t is

$$R = 1 - \int_0^t f(t)dt = e^{-\int_0^t m(t)\, dt} = e^{-\int_0^t \phi A\, dt} \tag{32}$$

where (in meteoroid technology) ϕA is flux ϕ times exposed area A. Any procedural convenience to be gained in the determination of R in Eq. 32 will depend essentially on the convenience of evaluating the integral of m(t); but, as Toralballa [39] has shown, the specific mortality function corresponding to the Poisson distribution function is the constant reciprocal of the mean-time-to-occurrence for the repeated event; i.e., m is the average rate of occurrence of the event, or in meteoroid technology, flux ϕ times exposed area A, and Eq. 32 becomes

$$R = e^{-\phi A t}. \tag{33}$$

SECTION III. INTERPRETATION OF THE AVAILABLE INFORMATION

A. METEOROID FLUX

1. Temporal Dependence of Flux. As McCoy [29] states "historically, celestial debris has been classified as either 'shower' (swarms and streams) or 'sporadic'. Any meteor that could not be identified with a stream or swarm was classified as sporadic. For meteors in the visual range, several investigators have shown a preponderance (60-95%) to be sporadic; Lovell has estimated 80-90% sporadic for all meteor sizes."

Davison and Winslow [12] state that shower meteors make up about 20-30% of the meteors sighted; and they cite several references to the effect that "The peak activity during these showers may be 4 to 5 times the sporadic meteor rate, but on extremely rare occasions much greater."

Ellyett and Keay [18] have shown some data which may indicate a significant variation in hourly meteor rate throughout the day and in daily rate throughout the year "...expected as a result of the tilt of the earth's axis, causing a hemispherical autumnal maximum and vernal minimum." Also Dubin [15] in an analysis of meteoritic impact data on artificial satellite Explorer I (1958α) says that, after discarding 16 of the first 88 hits, "A diurnal dependence, resulting by the earth's heliocentric velocity, is evidenced, in that nearly 90% of the 72 hits shown ... occurred on the dawn side of the earth between the hours of midnight and twelve noon." Hibbs [22 and 23] has subsequently given a different interpretation of the data (Section III. A. 3), but failed to convince Dubin [16].

Bel'kovich [4] in reporting analytical and experimental investigation of the Poisson distribution hypothesis for "... the chance recording of a meteor, at a radar station or during visual observations ..." concluded: "The distribution of the number of meteors in time follows the Poisson law and is independent of the size of the observational time interval and of the presence of showers." In his same report Bel'kovich [4] also said: "The distribution of the number of recorded meteors in time will not be stationary since observational

conditions are continuously changing owing to the earth's daily rotation and motion along its orbit." Perhaps what Bel'kovich means by the above two statements is that the rate will change but that one can predict neither when the change will occur nor what the rate will be after it has changed.

But in Eq. 33 different values of ϕ may be forecast for different time intervals, as by histogram representation. One can then see that a non-Poisson situation can be approximated as piece-wise Poisson, for ϕ is piece-wise constant. Then, instead of Eq. 33,

$$R = e^{-A\left[\phi_1(t_1 - t_0) + \ldots + \phi_n (t_n - t_{n-1})\right]} \tag{34}$$

for $t = t_n - t_0$.

It should be emphasized, however, that Eqs. 33 and 34 give the same result for the same exposure At whenever ϕ in Eq. 33 is the time average of the $\phi_1, \ldots, \phi_n$ in Eq. 34. It does not make any difference whether or not the ϕ in Eq. 33 and the $\phi_1, \ldots, \phi_n$ in Eq. 34 are further resolved into: (1) components due to sporadic meteoroids, and (2) components due to shower meteoroids - unless it should be found that the two populations should be separately described with respect to mass, density, velocity, etc.

2. Directional Dependence of Flux. Dubin [15] writes that "Because the earth is shielding the satellite, the impact rate for the same mass component of micrometeorites at one astronomical unit is nearly twice this [detected] value...". Whipple [41] writes with appropriate caution: "A correction for distance above the earth's surface is rather difficult to apply unless the precise orbital characteristics of the incoming meteoric bodies are known. Perhaps the inclusion of the factor $\frac{1}{2}$ is adequate for the ordinary problem near the earth's surface. At extreme distances, greater than 10^4km, a complete recalculation is needed with very careful attention to the orbital characteristics of meteoroids in space and of the space vehicle in question. Even after correction for the factor $\frac{1}{2}$, the number striking the vehicle will probably fall off with increasing distance from the earth."

According to Siedentopf [37]: "The particles entering the earth's atmosphere [meteor observations] have very eccentric orbits, whereas most particles that are optically effective move in nearly circular orbits under the action of the Poynting-Robertson effect. The

observable meteors generally have radii greater than 100μ, whereas the brightness of the zodiacal light and the Fraunhofer corona comes mainly from the particles with radii between 1 and 100μ." Also Ehricke [19] says: "According to Takaknbo the radius of the dust particles most effective in the zodiacal light and the F corona is about 20μ."

McCoy [29] reports: "These sporadic particles enter the earth's atmosphere from all directions, within approximately ±25° of the ecliptic, and at irregular intervals. It has been observed through analysis of radiant points that the ratio of meteors approaching the earth from behind to those approaching from ahead is close to 30:1. This is because most meteors have direct orbits like the earth rather than retrograde motion. However, the true ratio of direct to retrograde orbit meteors is approximately 50:1. The difference in ratios is explained by the fact that the earth overtakes some of the slower meteors. Also, because of the earth's orbital velocity more meteoric encounters (~2:1) occur on the leading or forward face, as can be readily substantiated by observing the increased number of visual displays after midnight than before."

Davison and Winslow [13] show a graph (which they credit to Lovell) for the distribution of visual sporadic meteor radiants in ecliptic latitude which supports the estimate that approximately 50% are inclined within ±15° of the ecliptic. And in two other graphs (which they credit to Hawkins [51]) they [12 and 13] show: (1) "Polar diagram drawn in the plane of the earth's orbit which shows the apparent number of meteor radiants detected per unit angle, per unit time" and (2) "Polar diagram drawn in the plane of the earth's orbit which shows the number of meteors per unit angle which cross earth's orbit per unit time." Those two graphs, reproduced from Hawkins' [51] paper, are included in this report as Figs. 15 and 16. They show clearly the predominant proper motion of the meteoroids and the tendency for the earth to overtake the meteoroids. Davison and Winslow [12] rightly remark, "It could be concluded, therefore, that the preferred orientation of a [spacecraft's exposed] surface is parallel to the plane of the ecliptic with the major axis parallel to the apex of the earth's way."

If the spacecraft is to have attitude control, then part of its area, A_1, will be so located and oriented that the meteoroid flux with respect to it is ϕ_1, and similarly for A_2 with ϕ_2, etc.; so that, instead of Eq. 33, it would follow from Eq. 32 that

$$R = e^{-t(\phi_1 A_1 + \ldots + \phi_n A_n)}. \qquad (35)$$

3. Spatial Dependence of Flux. Nazarova [31] concluded: "If one compares the results obtained from experiments with Sputnik III and the three Soviet space rockets, it will be seen that the density of meteoric matter in the vicinity of the earth is not constant. It varies in time and space."

After some analysis of the micrometeoroid-impact sonic data from Sputnik III (1958 δ_2), Nazarova [32] concluded "... that the number of impacts varies with changes in the position of the satellite in its orbit but not with changes in altitude." And subsequently, in interpreting the micrometeoroid-impact sonic data from Explorer VIII (1960 ξ), McCracken, et.al. [30], similarly concluded "... that available direct measurements show no discernible evidence of an appreciable geocentric concentration of interplanetary dust particles."

But that meteoroid flux should be accentuated in the vicinity of a planet, aside from the shadowing effect discussed in Section III.A.2., should be expected because it can be shown analytically that, for hyperbolic trajectories of meteoroids passing planets, the partial derivative of radial distance of closest approach with respect to the projected (i.e., gravity-free) miss distance is both positive and less than unity. In regard to this phenomenon, the author has gone no further than to this qualitative verification, but Beard [3] writes: "The overall effect of the dust blanket at the surface of the earth will be to increase the concentration of dust, calculated in the absence of the earth's gravitational field, by a factor possibly as large as 6000, depending on the eccentricity of the dust's orbits. (The factor [Beard says] is more likely about a few hundred.) ...A third of this blanket is concentrated within one earth radius of the earth's surface ... A simple approximate calculation of the dust orbit in the gravitational field of the sun and a planet reveals that the concentration of the dust varies inversely with the three-halves power of its distance from the center of the planet." But one suspects that the radial dependence of meteoroid flux must also be functionally related to the mass of the particular planet.

That meteoroid flux in the vicinity of a planet may be radial-distance dependent is further suggested by capture processes other than direct collision. In 1958 Baker [2] reported: "Preliminary calculations show that only about 0.2% of the total number of the porous stony meteorites which strike the earth will result in natural satellites

...[which]... would originate from 'near-miss' meteoritic trajectories that only graze the atmosphere of the earth, the meteorites being slowed sufficiently to enter onto a geocentric elliptical orbit...It is noted that there are other [further] mechanisms for capture of natural satellites involving the attraction of the moon, the Poynting-Robertson effect, and so on..." By including data which had been earlier discarded by Dubin [15], as discussed in Section III.A.1., Hibbs [22] gave this interpretation to the micrometeoroid-impact data from artificial satellite Explorer I: "The distribution in longitude relative to the satellite-earth-sun angle corresponds to an altitude distribution and apparently contains no information that is not better shown in this latter distribution. With suitable analysis, the altitude distribution yields information on the velocity of the particles relative to the center of the earth. The conclusion is that the average particle measured by Explorer I was in a closed orbit around the earth rather than on an impact trajectory from a great distance to the surface of the earth." As each captured particle would repeat many orbits, supposedly the 0.2% captures, quoted above from Baker [2], would be sufficient to support a considerable steady-state population of captured particles. These findings by Hibbs are further supported by those later reported by Laevastu and Mellis [27]: "The estimates of the rate of fall of cosmic spherules to the earth, based upon the counts from sediments, depend, among other things, on the exact determination of the rate of sedimentation. As the value calculated from satellite data is considerably higher, it gives added support to the conclusions of Hibbs..."

Aside from the above hypothesized increase in meteoroid flux in the vicinities of the planets, there are further observational evidences that meteoroid flux increases with decreasing distance from the ecliptic and from the sun. Beard [3] says: "The dust diffracts sunlight at small angles which may be observed in the solar corona during solar eclipses. Sunlight is also reflected by the dust at large angles which may be observed as ... zodiacal light." This interpretation of solar corona and zodiacal light data is further supported by the in-fall theory of cosmology; e.g., (1) Beard [3] says: "The relativistic interaction of these particles with sunlight, as shown by Robertson and Wyatt and Whipple, causes them to spiral slowly into the sun with a radial velocity inversely proportional to the solar distance ... One further factor that determines the radial distribution of interplanetary dust is the gravitational attraction of the planets... which causes the dust to approach the plane of the ecliptic with a drift velocity that is inversely proportional to the square root of the solar distance.

Inclusion of this effect results in a dust concentration in the ecliptic plane that is inversely proportional to the three-halves power of the solar distance," and (2) Best [5] says: "Supposing the solar system encountered such a cloud [of interstellar dust at a relative velocity corresponding to the 20 km/sec solar proper velocity], the particles would all have hyperbolic orbits with respect to the sun. However, the orbits do not remain hyperbolic of fixed eccentricity due to the braking force of solar radiation, which for initially elliptical orbits leads to the Poynting-Robertson effect, and the eccentricity will decrease near the sun ... Note that [the criterion for capture by retardation by solar radiation] is identical with [the criterion for the Lyttleton cometary accretion process] and thus if either capture process is involved the capture radius will be about 5 A.U., which is just inside the orbit of Jupiter."

4. Mass Dependence of Flux. So as not to have to be concerned further in this report with the directional aspects of meteoroid flux, one can assume that the term is used in the same sense as Whipple [41] used it: the meteoroid flux encountered by a sphere in a near-earth orbit is the number per unit time hitting the sphere divided by the area of the effectively exposed hemisphere. And, as Rodriguez [35] suggests: "An equation of the form

$$F_{>} = \alpha_1 m^{\beta_1} \tag{36}$$

is used by many investigators. $F_{>}$ is the [flux] of particles having mass m or greater, and α_1 and β_1 are empirical constants."

The selection of a solution pair of values (α_1, β_1) is not decided in the ($F_{>}$, m) domain by most authors, excepting Laevastu and Mellis [27]. It is decided in the ($\log_{10} F_{>}$, $\log_{10} m$) domain; i.e., from a family of equi-probable contours of possible solution points which, through Eqs. 16 through 29, are the consequences of the following underlying functional representation

$$\log_{10} F_{>} = \beta_1 \log_{10} m + y_1 \tag{37}$$

where β_1 is a constant and y_1 is an approximately normally distributed random variable with mean $\overline{y}_1$ and standard deviation σ_{y_1}. This Eq. 37 and such other functional representations as will be used in this report to represent uncertain quantities and/or relations are intended as expedients for the propagation of confidence through other functions of this and other uncertain parameters.

Functional relations between the flux $F_>$ of meteoroids, with masses equal to or greater than m, to be encountered by a spacecraft in orbit near the earth, or relations between $\log_{10} F_>$ and $\log_{10} m$, have been inferred primarily from data obtained by careful quantitative measurements of physical parameters involved in the following four phenomena: (1) the interaction of meteoroids with the atmosphere of the earth as studied by visual, photographic, and radar methods and discussed (e.g.) by Whipple [41], (2) the accumulation of meteoroid debris on the earth as studied by chemical, physical, and statistical analyses of the sediments and discussed (e.g.) by Laevastu and Mellis [27], (3) the disturbance by micrometeoroids hitting instrumented artificial satellites as studied by microphones and discussed (e.g.) by Dubin [14 and 15], and (4) interaction between micrometeoroid and electromagnetic radiation as inferred by physical optical peculiarities of solar corona and zodiacal light and discussed (e.g.) by Beard [3]. The combined interpretation of these four separate categories of information is further facilitated (or confused, depending on one's point of view) by theoretical considerations of the paths of meteoroids, of given mass and cross-sectional area, moving under the combined influences of solar radiation and solar and planetary combined gravitational fields - as discussed (e.g.) by Siedentopf [37], Best [5], and Beard [3].

The various published interpretations of the information described above differ considerably, and in other ways also suggest that the results must yet be uncertain to a considerable extent. When various interpretations are considered as points in a graph, $\log_{10} F_>$ versus $\log_{10} m$, then results are missing for 10^{-7} gm $< m <$ 10^{-4} gm. Except for the degradation of optical surfaces, thin films, paints, etc., this is the entire region of interest - mass m possibly large enough for penetration of a space vehicle (or vital component) and flux $F_>$ possibly too high to be ignored. Also not a single one of the various phenomena or underlying principles of interpretation gives points on both sides of the interval of interest.

Concerning visual, photographic and radar tracking of meteors, Nazarova [32] says: "At present [1960] . . . these methods are only useful for registering particles with masses of 10^{-4} gm and more." For this side of the region of interest, Whipple [41] suggests: ". . . an increase in the number of meteoroids inversely as the mass of the particle." This is equivalent to assuming a unit value of $-\beta_1$ in Eq. 37.

By taking the antilogarithm of Eq. 37 one finds

$$F_{>} = m^{\beta_1} e^{(\log_e 10)\, y_1} \tag{38}$$

which (except for the constant factor) is the same functional form as Eq. 23 with

$$\beta = \log_e 10 = 2.303 \ . \tag{39}$$

Therefore Eqs. 23 through 29 are applicable here; and Whipple's [41] tabulated data imply that

$$\bar{y}_1 = -12.20 - \Delta y_1 \tag{40}$$

where Δy_1 is a component which would correct any bias in m_0 in Eq. 42.

About the micrometeoroid side of the region of interest, Bjork [6] says: "... At the present time [May 1960], rocket and satellite experiments are inherently limited to measuring the impacts of meteoroids having masses of about 10^{-8} gm or less." By McCracken, Alexander, and Dubin's [30] more recent interpretation of Explorer VIII results, Eq. 37 is approximately true for $10^{-10} < m < 10^{-6}$ gm when

$$\beta_1 = -1.70$$

and

$$\bar{y}_1 = -17.0$$

Bjork [6] recommends a relation, to fit both the satellite and radar data regions, which similarly implies that

$$\beta_1 = -10/9$$

and

$$\bar{y}_1 = -12 \ .$$

Nysmith and Summers [33] gave a summary of results from ten different satellite determinations of β_1 and y_1 in Eq. 37 with mass sensitivities in the interval $10^{-10} < m \leq 2 \times 10^{-8}$ gm and with an average

value of -8.70 for the common logarithm of the mass sensitivity limit. They preferred a unit value for $-\beta_1$, for comparison with meteor data, with which, by equally weighting their tabulated results,

$$\overline{y}_1 = -11.28$$

$$\sigma_{y_1} = 0.60 .$$

Beard [3] finds, from studies of solar corona and zodiacal light, that flux depends on radius to roughly the 3.5 power for small particles; implying that:

$$\beta_1 = -3.5/3 = -1.17 .$$

The establishment of a mathematical model which bridges the intermediate interval of extrapolation is not to be accomplished without considerable reservation. Laevastu and Mellis [27] say: "In making this extrapolation [from satellite data on small particles to larger particles], account is taken of the fact that essentially all cosmic particles $> 250\mu$ in diameter are intercepted by the planet Jupiter and therefore do not reach the earth." But since the volume of a sphere with 250μ diameter is 8.2×10^{-6} cubic centimeters, the mass must be within the interval $4 \times 10^{-7} \leq m \leq 3 \times 10^{-5}$ gm for density (Section III. C.) within the interval $0.05 \leq \rho \leq 3.6$. Also, about the small particles affecting solar corona and zodiacal light, Siedentopf [37] says: "A comparison of these results with the data obtained from meteor observations is difficult. The particles entering the earth's atmosphere have very eccentric orbits, whereas most particles that are optically effective move in nearly circular orbits under the action of the Poynting-Robertson effect. The observable meteors generally have radii greater than 100μ whereas the brightness of the zodiacal light and the Fraunhofer corona comes mainly from the particles with radii between 1 and 100μ. So the information gained by optical methods and by meteor observations covers different aspects of the interplanetary matter that practically do not overlap." Interestingly enough, these apprehensions support the notion that for the high-flux region, say $F_> > 10^{-7}$ particles per square meter per second, the results of McCracken, Alexander, and Dubin [30] may be appropriate; whereas Whipple's [41] results may be appropriate for lower flux values. This would be equivalent to assuming that there are no meteoroids with masses in the interval

$$10^{-(17.0 - 7.0)/1.7} = 1.3 \times 10^{-6} < m < 10^{-(11.88 - 7.00)} =$$

$$= 1.3 \times 10^{-5} \text{ gm} \qquad (41)$$

because they have been captured by the major planets. It appears to be more likely that the available information on either side of the region of extrapolation is not sufficiently firm to warrant interpretations such as Eq. 41.

Now consider the accuracy of the data for the larger meteoroids. As the basis for his analysis, Whipple [41] says, "... a meteor of visual magnitude zero is determined to have a mass of the order of 25 gm." Bjork [6] says that Whipple "... has calculated m_0 lies between 1 and 30 gm with 25 gm the preferred value."

In the physical theory of meteors, as presented by Öpik [44], Kallmann [45], Levin [46], and Jacchia [47], the expressions for meteoroid mass m, as related to visual magnitude, are always found by taking the antilogarithm of a linear expression for $\log_{10} m$, for which the slope and intercept are both somewhat random and problematical and, the present state of the information being such as it is, might just as well be assumed to be normally distributed. This is part of the basis for the contention that y_1 can be considered to be approximately normally distributed; but also it shows that values of m_0 bear the Eq. 29 relation to confidence. Then the 25 gm value for m_0 is a result of choice rather than of skewness; the value otherwise implicated being

$$m_0 = 10^{\frac{1}{2}(\log_{10} 30 + \log_{10} 1)} = 5.48 . \qquad (42)$$

In discussing McCrosky's interpretation of his experiments using simulated meteors to estimate luminous efficiency, Davison and Winslow [12] stated McCrosky indicated that luminous efficiency from 3 to 100 times as large as that used by Whipple was not precluded by the experiment. The common logarithm of such a correction factor would be the further bias which would have to be algebraically subtracted from y_1 in Eq. 37; because Whipple [41] says: "It is assumed that the mass decreases by a factor of $10^{0.4}$ per magnitude step..." while a unit increase in visual magnitude corresponds also to a luminous intensity decrease by a factor of $10^{0.4}$. Therefore, the bias in y_1 corresponding to a luminous efficiency correction factor of $25/m_0$ is

$$\Delta y_1 = \log_{10}(25/m_0) \tag{43}$$

The question of what value to use for m_0 is related to the km/sec meteoroid velocity v_a by Öpik [44] as follows:

$$\log_{10} m_0 = 10.97 - 1.7 \log_{10}(10^5 v_a) .$$

This Eq. 43 implies that m_0 is 1.02 or 0.70 gm depending on whether one uses 28 km/sec for v_a, as Whipple [41] does for all visual magnitudes up to 7, or 35 km/sec, as will be shown in Section III. B. to be more nearly deducible from mass versus velocity relations.

When all of the above reasons are considered, the author prefers to use the Eq. 42 value for m_0; then by Eqs. 40, 42, and 43,

$$\overline{y}_1 = -12.86 . \tag{44}$$

Also by the reasons already discussed in this section, it follows that when -8.70 is the mean of the common logarithm of the mass sensitivity limits for the satellite data, as discussed above, then the median mass for the detected micrometeoroids will be approximately

$$10^{-8.70 + (-\beta_1)^{-1} \log_{10} 2} \text{ gm} = m_s \tag{45}$$

at which value for m one has also implied that

$$\log_{10} F_> \Big|_{m_s} = 8.70 + (\beta_1)^{-1} \log_{10} 2 - 11.28 =$$

$$= -2.58 + 0.301 (\beta_1)^{-1} . \tag{46}$$

But by Eqs. 37 and 44 one has also implied that, at the same value of m,

$$\log_{10} F_> \Big|_{m_s} = \beta_1 [-8.70 - 0.301 (\beta_1)^{-1}] - 12.86 =$$

$$= -8.70\beta_1 - 13.16 . \tag{47}$$

The simultaneous solution of Eqs. 46 and 47 is

$$\beta_1 = -1.19 \tag{48}$$

which agrees very well with the -1.17 value, mentioned above, based on Beard's [3] estimate.

Nothing has been said about the confidence value which should be associated with the above mentioned delimitations: $1 < m_0 < 30$ gm, but presumably it is intended that they are each separated from the 50% confidence value for m_0 by not less than one probable error of m_0; i.e.,

$$\sigma_{y_1} = 0.50\,(\log_{10} 30)(0.6745)^{-1} = 1.10 \ . \qquad (49)$$

In deciding whether this Eq. 49 estimate for σ_{y_1} is too much in excess of the value 0.60 mentioned above, one must consider further the various uncertainties besetting the determination of the masses of micrometeoroids based on data from instrumented satellites and from other sources.

The mass dependence of micrometeoroid flux for $m \leq 10^{-7}$ gm, as inferred from microphone impulses from instrumented satellites, also has considerable possibility for error. In reporting Explorer I results, Dubin [15] says: "It was also assumed that since the micrometeorite detector on 1958α was sensitive to the momenta of the impacts to velocities as high as 4 km/sec, the momentum transfer remained proportional to the first power of the velocity of impact at meteor velocities. If this is not basically correct, the error may become large at the high end of the velocity distribution . . . It was further assumed that all impulses measured were meteoritic impacts." Elsewhere, Dubin [14] says: "The velocities of meteoroid impacts upon a satellite may vary between 10 km/sec and 70 km/sec. . ." and says further that, according to computations by Bjork, at 70 km/sec the vehicle experiences a change in momentum which is ". . . two and one-half times the initial particle momentum." More recently McCracken, Alexander, and Dubin [30] report that the calibration has been extended through speeds up to approximately 10 km/sec and that: "An average velocity of 30 km/sec, relative to a satellite has been assigned to the dust particles in order that the data may be used to determine the average mass distribution. . ." And, in inferring the mass of micrometeoroids from the impulses from microphones in Sputnik III, Nazarova [31 and 32] used a similar relationship ". . . while assuming that the mean velocity of the particle is equal to 40 km/sec. . ." But Whipple [41] says: "Undoubtedly the velocity falls off for smaller meteoroids as we deal more and more with particles whose orbital eccentricities and dimensions have been reduced by physical effects. . ." and for $m \leq 10^{-7}$ gm he assumed an

average velocity of 15 km/sec. Also Öpik [43] infers that a velocity distribution with mean velocity and standard deviation equal to 14.5 and 2.4 km/sec respectively implies a frequency distribution of particle diameters which is in good agreement with the distribution of diameters found by Laevastu and Mellis [43] for "extraterrestrial material in deep-sea deposits." Öpik [43] concluded that: "A low value of and a low dispersion in the velocities is definitely indicated, corresponding to cosmic dust circling the sun in direct orbits of low eccentricity." It does seem possible, therefore, that any bias due to a proportionately larger transfer of momentum above the calibration velocities may compensate for any bias due to assuming higher average velocity. But with so much room for doubt, it seems appropriate to accept the Eq. 49 criterion for σ_{y_1}.

The author prefers to consider that, throughout the interval $10^{-10} < m < 10^{1}$ gm, meteoroid flux $F_>$ and mass m are related by Eqs. 29, 37, 44, 48, and 49 as illustrated graphically in Fig. 1 based on the Eq. 29 criteria.

B. METEOROID VELOCITY: MASS DEPENDENCE

1. Relative to the Earth's Atmosphere. Whipple [41] says: "A velocity of 28 km/sec is average for photographic meteors. Undoubtedly the velocity falls off for smaller meteoroids... The velocity at the edge of the earth's atmosphere cannot be less than 11 km/sec because of the earth's attraction... A mean value of 15 km/sec has been arbitrarily chosen for the smaller meteoroids and an arbitrary gradation of velocity with magnitude adopted." Thus, in his table, Whipple [41] indicated a velocity of 28 km/sec for all visual magnitudes less than or equal to 7, 15 km/sec for all visual magnitudes greater than or equal to 20, and otherwise a 1 km/sec decrease in velocity for each unit increase in visual magnitude. Also, in Section III.A.4. it was shown that Whipple [41] assumed that the mass decreases by a factor of $10^{0.4}$ per magnitude step, and therefore he implies a linear relation between velocity and $\log_{10} m$, which is apparently the basis for the illustration given by Nysmith and Summers [33]. In his tabulation, Whipple [41] further shows $3.96 \times 10^{-10} \leq m \leq 25.0$ gm for $27 \leq$ magnitude ≤ 0. But in the discussion leading up to Eq. 44, the decision was that the masses which Whipple assumed should be reduced by the factor $10^{-0.66}$; the above mass interval being thereby changed to $10^{-10.06} \leq m \leq 10^{0.74}$ gm. But if Whipple [41] had used, between magnitude 27 and 0, the same linear relation between magnitude and velocity which he assumed

between magnitudes 20 and 7, then the velocity would have been reduced nearly to the circular orbital velocity at magnitude 27, in agreement with Hibb's [22 and 23] analysis of micrometeorite data from instrumented satellites, and at magnitude 0 the 35 km/sec velocity would agree very nearly with the 35.5 km/sec average for the data for larger meteors attributed by Davison and Winslow [12 and 13] to Hawkins and Southworth. This would imply the following relation between the velocity, v_a (km/sec) and mass, m (gm):

$$v_a = (35 - 8)(\log_{10} 10^{0.74} - \log_{10} 10^{-10.06})^{-1} \log_{10} m +$$

$$+\left[8 - (35 - 8)(\log_{10} 10^{0.74} - \log_{10} 10^{-10.06})^{-1} (\log_{10} 10^{-10.06})\right] =$$

$$= 2.50 \log_{10} m + 33.2 \qquad (50)$$

for $10^{-10} \leq m \leq 10^{1}$ gm.

Dubin [15] refers to the cosmic dust detection limit of optical and radio measurements as "... approximately visual magnitude 10 ..." One wonders what the corresponding limit would be for the determination of meteoroid velocity at the edge of the earth's atmosphere -- evidently the magnitude limit would not be quite as high as it is just for detection. Whipple [41] says only: "Radio meteor studies may provide measures of the [velocity] gradation in the near future, perhaps to the twelfth magnitude."

By adjusting Whipple's [41] tabulated data for meteoroid masses, as discussed above, the relation between visual magnitude M and mass m is

$$m = 10^{0.74 - 0.40M} \qquad (51)$$

One can consider the average velocity of all meteoroids between the relatively infrequently occurring magnitude 0 and some higher magnitude $M_u \leq 10$ as a function of M_u. By Eqs. 37 and 50,

$$F_{>} = 10^{\beta_1 (0.74 - 0.40M) + y_1} \qquad (52)$$

Then by Eqs. 48 and 51, the number of meteors with $M \leq M_u$ is greater than the number with $M \leq M_u - 1$ by the following factor:

$$10^{-0.40\beta_1} = 3.00 .$$

Therefore the average velocity for meteors of magnitude $\leq M_u$ will be very nearly the same as the average velocity for those of a magnitude in the vicinity of M_u. On that basis one would expect that for Whipple's [41] data M_u is not appreciably higher than 7. No corresponding estimate is available for the above-mentioned data which gives velocity mean and standard deviation 35.5 and 13.3 km/sec respectively, but, assuming the Eq. 50 corresponding value of m, one has:

$$(m, v_a, \sigma_{v_a}) = (10^{0.92}\ \text{gm},\ 35.5\ \text{km/sec},\ 13.3\ \text{km/sec}). \tag{53}$$

Öpik's [43] theoretical distribution of cosmic dust velocities and diameters below 300μ gives velocity mean and standard deviation 14.5 and 2.40 km/sec respectively, and an average value of -6.99 for $\log_{10}(m/\rho)$. By taking the value of $\log_{10} m$ which, by Eq. 50, gives the 14.5 km/sec average velocity, one finds

$$(\log_{10} m, \log_{10} \rho) = (-7.48,\ -0.49 = \log_{10} 0.32) \tag{54}$$

i.e., $\rho = 0.32$ for small meteoroids. This agrees well with other results; e.g., Davison and Winslow [12] say: "Based on Beard's estimates [based on solar F-corona and zodiacal light] it would appear that the material density of these particles [1μ < diameter < 300μ] must be equal to or less than 0.3 gram per cubic centimeter." So one can agree that there is sufficient basis for another set of values:

$$(m, v_a, \sigma_{v_a}) = (10^{-7.48}\ \text{gm},\ 14.5\,\text{km/sec},\ 2.40\,\text{km/sec}) . \tag{55}$$

But the following Eq. 56 functional relation

$$\log_{10} v_a = \beta_2 \log_{10} m + y_2 \tag{56}$$

where β_2 is a constant and y_2 is an approximately normally distributed random variable with mean $\overline{y}_2$ and standard deviation σ_{y_2}, will more appropriately represent the Eqs. 53 and 55 information, than will one like Eq. 50, because: (1) σ_{y_2} decreases as v_a decreases, and (2) values of v_a must not be too severely depressed as m decreases.

By applying Eq. 7 to Eq. 56 and using the Eqs. 53 and 55 information,

$$\sigma_{y_2} = \sigma_{\log_{10} v_a} = (\sigma_{v_a} / v_a) \log_{10} e$$

$$= (13.3/35.5) \log_{10} e = 0.163 \Big\} \text{ independent estimates}$$

$$= (2.40/14.5) \log_{10} e = 0.072 \Big\} \text{ with mean:}$$

$$= \tfrac{1}{2} (0.163 + 0.072) = 0.12 \quad . \tag{57}$$

By Eqs. 29 and 56, it follows also from the information of Eqs. 53 and 55 that

$$\log_{10} 35.5 = \beta_2 \log_{10} 10^{0.92} + \bar{y}_2 \tag{58}$$

$$\log_{10} 14.5 = \beta_2 \log_{10} 10^{-7.48} + \bar{y}_2 \tag{59}$$

Then by simultaneous solution of Eqs. 58 and 59,

$$\beta_2 = 0.046 \tag{60}$$

$$\bar{y}_2 = 1.51 \quad . \tag{61}$$

The results from Eqs. 57, 60, and 61 for σ_{y_2}, β_2, and $\bar{y}_2$ respectively when used in Eq. 56 with the criteria from Eq. 29 for contours of equi-probable values of v_a versus m, seem to represent very well the available information throughout the interval $10^{-10} < m < 10^{1}$ gm, as illustrated graphically in Fig. 2.

2. Relative to a Vehicle in a Near-Earth Orbit. As the earth orbits around the sun, the gravitational field of the earth deflects toward the earth the meteoroids which otherwise, in their elliptical orbits around the sun, would merely pass close by the earth.

The distribution of closing velocities between the meteoroids and a space vehicle in orbit near the earth will depend on the distribution of angular deviations of the local vertical from the tangents to the meteoroid trajectories at the point of impact. It is assumed: (1) that the result will be approximately the same if a two-body meteoroid-earth model is substituted for the more nearly correct three-body meteoroid-sun-earth model, and (2) that, just as meteoroid velocity with respect to the earth's atmosphere can be related to mass by Eq. 56, closing velocity v_c with respect to a space vehicle in orbit near the earth can be similarly related by

$$\log_{10} v_c = \beta_3 \log_{10} m + y_3 \tag{62}$$

where β_3 is a constant and y_3 is an approximately normally distributed random variable with mean $\bar{y}_3$ and standard deviation σ_{y_3} representing uncertainty of the relation physically and according to available information.

The necessary functional relations for hyperbolic trajectories are given in introductory treatments of celestial mechanics [e.g., 19]. The hyperbolic velocity excess v_∞ is

$$v_\infty = (v_a^2 - 2\gamma m_e / r_a)^{\frac{1}{2}} \tag{63}$$

where m_e is the mass of the earth, γ is the universal constant of gravitation, and r_a is the radial distance from the center of the earth to the zone implicit in meteoroid velocity data discussed above. The velocity v_r at radial distance r is, by Eq. 63

$$v_r = \left[v_a^2 - 2\gamma m_e \left(\frac{1}{r_a} - \frac{1}{r}\right)\right]^{\frac{1}{2}}. \tag{64}$$

Because a spacecraft is orbiting at geocentric radial distance r, it is convenient to consider that a geocentric sphere of radius r is making a tunnel of radius $D_{\frac{1}{2}\pi}$ through a swarm of meteoroids; where: (1) the trajectory of any meteoroid originally approaching along the surface of the tunnel with the closing velocity v_∞ will be tangent to the sphere r, and (2) the trajectory of any meteoroid originally approaching with the same velocity but within the tunnel and displaced only $D_{x_1} < D_{\frac{1}{2}\pi}$ from the tunnel axis will cut the sphere r at angle $x_1 < \frac{1}{2}\pi$ with respect to the local position vector (i.e., x_1 is the zenith angle). Because of the conservation of angular momentum, the dot product of the meteoroid velocity vector and geocentric radius vector is invariant with respect to the position of any particular meteoroid along its trajectory; i.e.,

$$v_\infty D_{x_1} = v_r r \sin x_1 \tag{65}$$

Therefore, by Eqs. 63 through 65,

$$\sin x_1 = (1/r) D_{x_1} \left[\frac{r_a v_a^2 - 2\gamma m_e}{r_a v_a^2 - 2\gamma m_e (1 - r_a/r)}\right]^{\frac{1}{2}} = D_{x_1} / D_{\frac{1}{2}\pi}. \tag{66}$$

Then by Eq. 66, the tunnel radius is

$$D_{\frac{1}{2}\pi} = r\left[\frac{1 - 2\gamma m_e(1 - r_a/r)/r_a v_a^2}{1 - 2\gamma m_e/r_a v_a^2}\right]^{\frac{1}{2}}. \tag{67}$$

Although the above tunnel concept was convenient in the derivation of Eqs. 66 and 67, it should be emphasized that the results are valid also when meteoroids approach the earth from all directions as they do in practice; e.g., by Eq. 66 one sees that half of the meteors should approach the atmosphere with angles deviating less than 45 degrees from the zenith.

When a spacecraft is orbiting in a nearly circular orbit with geocentric coordinate r, then its velocity v_s is essentially horizontal with

$$v_s = (\gamma m_e/r)^{\frac{1}{2}} . \tag{68}$$

Then, when one assumes that both the meteoroid and space vehicle are moving in the same plane, it follows from Eqs. 64, 66, and 68 that the closing velocity v_c is

$$v_c = \left[(v_s + v_r \sin x_1)^2 + (v_r \cos x_1)^2\right]^{\frac{1}{2}} =$$
$$= \left[v_s^2 + v_r^2 + 2v_r v_s \sin x_1\right]^{\frac{1}{2}} \tag{69}$$

Because the relative area of a narrow concentric ring in the cross-section of the tunnel is equal to the product of its relative circumference and its differential relative width, and because one must admit equal probability for positive and negative values of x_1, it follows from Eq. 66 that the probability distribution function for x_1 is

$$f(x_1) = \left|(2\pi \sin x_1)\frac{d}{dx_1}(\sin x_1)/2\pi\right| = \tfrac{1}{2}\left|\sin 2x_1\right| . \tag{70}$$

By Eqs. 2 and 70

$$\overline{x_1} = 0. \tag{71}$$

By Eqs. 5 and 70

$$\sigma_{x_1} = \left[(\pi^2 - 4)/8\right]^{\frac{1}{2}} \tag{72}$$

By Eqs. 2 through 4, 69, and 70, the expected value of v_c^2 is

$$E\left[v_c^2\right] = v_s^2 + E\left[v_r^2\right] . \tag{73}$$

But because the closing velocity v_c is increased from v_r by only a relatively small increment due to v_s, Eq. 73 can be appropriately approximated and, with Eqs. 64 and 68, simplified by

$$\bar{v}_c = (v_s^2 + \bar{v}_r^2)^{\frac{1}{2}} = \left[v_a^2 + (\gamma m_e/r)(3 - 2r/r_a)\right]^{\frac{1}{2}} . \tag{74}$$

By Eq. 7, by taking the standard deviation of v_c in Eq. 69, and then by applying the relations from Eqs. 64, 68, 71, 72, and 74,

$$\sigma_{v_c} = \left[\left(\frac{\partial v_c}{\partial v_r}\frac{\partial v_r}{\partial v_a}\sigma_{v_a}\right)^2 + \left(\frac{\partial v_c}{\partial x_1}\sigma_{x_1}\right)^2\right]^{\frac{1}{2}} =$$

$$= \frac{1}{v_c}\left[(v_a\sigma_{v_a})^2 + (v_r v_s \sigma_{x_1})^2\right]^{\frac{1}{2}} =$$

$$= \left[(v_a\sigma_{v_a})^2 + (v_r v_s \sigma_{x_1})^2\right]^{\frac{1}{2}} \left[v_s^2 + v_r^2\right]^{-\frac{1}{2}} =$$

$$= \left[v_a^2(\sigma_{v_a}^2 + \sigma_{x_1}^2 \gamma m_e/r) - 2(\gamma m_e/r)^2 (r/r_a - 1)\sigma_{x_1}^2\right]^{\frac{1}{2}}$$

$$\left[v_a^2 + (\gamma m_e/r)(3 - 2r/r_a)\right]^{-\frac{1}{2}} \tag{75}$$

Levin [46] says that 6740 km is the radius of the atmospheric layer in which meteors are observed. Then for a space vehicle in orbit near the earth, say at (6378 + 500) km,

$$(\gamma m_e/r)^{\frac{1}{2}} = (\gamma m_e/r_a)^{\frac{1}{2}} = 7.91(6378/6878)^{\frac{1}{2}} = 7.62\,\text{km/sec} . \tag{76}$$

With Eqs. 72 and 76, Eqs. 74 and 75 become

$$\bar{v}_c = \left[\bar{v}_a^2 + (7.62)^2\right]^{\frac{1}{2}} \tag{77}$$

$$\sigma_{v_c} = \left\{\bar{v}_a^2\left[\sigma_{v_a}^2 + (7.62)^2\left(\frac{\pi^2 - 4}{8}\right)\right]\right\}^{\frac{1}{2}} (\bar{v}_c)^{-1} . \tag{78}$$

These Eqs. 77 and 78 results, together with Eq. 62 and the Eqs. 3 and 7 operations, lead to the following Eqs. 79 and 80 relations:

$$\beta_3 \log_{10} m + \bar{y}_3 = \log_{10}\left[v_a^2 + (7.62)^2\right]^{\frac{1}{2}} \tag{79}$$

$$\sigma_{y_3} = \sigma_{\log_{10} v_c} = (\sigma_{v_c}/v_c) \log_{10} e =$$

$$= v_a (\log_{10} e) \left[\sigma_{v_a}^2 + (7.62)^2(\pi^2 - 4)/8\right]^{\frac{1}{2}} \left[v_a^2 + (7.62)^2\right]^{-1} . \quad (80)$$

The following Eqs. 81 and 82 are found by substituting the information from Eqs. 53 and 55 into Eq. 79:

$$\beta_3 \log_{10} 10^{0.92} + \bar{y}_3 = \log_{10}\left[(35.5)^2 + (7.62)^2\right]^{\frac{1}{2}} \quad (81)$$

$$\beta_3 \log_{10} 10^{-7.48} + \bar{y}_3 = \log_{10}\left[(14.5)^2 + (7.62)^2\right]^{\frac{1}{2}} . \quad (82)$$

By solving Eqs. 81 and 82 simultaneously, one finds the following numerical values for β_3 and $\bar{y}_3$:

$$\beta_3 = 0.041 \quad (83)$$

$$\bar{y}_3 = 1.52. \quad (84)$$

The following Eqs. 85 and 86 are found by substituting the information from Eqs. 53 and 55 into Eq. 80:

$$(v_a, \sigma_{v_a}, \sigma_{y_3}) = (35.5, 13.3, 0.173), (14.5, 2.40, 0.168) \quad (85)$$

$$\sigma_{y_3} = \tfrac{1}{2}(0.173 + 0.168) = 0.17 . \quad (86)$$

The results from Eqs. 83, 84, and 86 for β_3, $\bar{y}_3$, and σ_{y_3} respectively, when used in Eq. 62 together with the Eq. 29 criteria for contours of equi-probable values of v_c versus m, seem to represent very well the available information throughout the interval $10^{-10} < m < 10^{1}$ gm, as illustrated graphically in Fig. 3.

C. METEOROID DENSITY: MASS DEPENDENCE

Meteoroids differ not only in mass, but also those which have approximately the same mass may differ widely in composition and structure. They are, in the order of increasing abundance and decreasing puncturability, classified broadly as: (1) metallic, with density somewhat more or less than that of iron, say $\rho = 7.8$, (2) stony, say with density somewhat more or less than $\rho = 3.5$, and (3) fluffy,

with density sometimes said to be somewhat more or less than $\rho = 0.05$. Whipple [41] says: "... the meteoric bodies, or meteoroids, manifested as ordinary meteors are extremely fragile and breakable." So presumably none of the fluffy meteoroids of appreciable size would have sufficient integrity to survive through the atmosphere and be recovered from the earth's surface. Then one may further presume that it is only with respect to metallic and stony meteoroids that one may apply Holl's [26] comment: "From the analysis of nearly 1000 meteorites recovered from the earth's surface, it has been determined that dielectric particles are nearly ten times as numerous as metallic ones."

Whipple [41] says: "The evidence is extremely strong, although not quite conclusive, that the density of ordinary meteoroids is the order of $0.05\,gm/cm^3$. This value depends, to a limited extent, upon physical arguments from photographic meteor data..." But one is somewhat at a loss for an interpretation of "...is the order of..." This can more appropriately be decided after reviewing the discussion in Section III.A.4. about the possibility that, as Davison and Winslow [12] attribute to McCrosky, the luminous efficiency for meteors may be from 3 to 100 times as large as that used by Whipple. Davison and Winslow [12] say further that: "An increase of 100 in the efficiency would have two ramifications. It would decrease the mass associated with a particular meteor sighting by a factor of 100 and increase the particle density for spherical particles by a factor of 10." Apparently the functional relation between density ρ and mass m, which has to represent both physical fact and the extent of information about it, might be represented by:

$$\log_{10}\rho = \beta_4 \log_{10} m + y_4 \tag{87}$$

where β_4 is a constant and y_4 is an approximately normally distributed random variable with mean $\overline{y}_4$ and standard deviations σ_{y_4}. Because of the $(25/5.48 = 4.56)$ meteor luminous efficiency correction factor (in the interval $3 < 4.56 < 100$), the choice for which has already been supported in Section III.A.4., Whipple's above estimate of the density of "ordinary meteoroids" must be transformed to

$$(v_a, \rho) = [28\ km/sec,\ 0.05\,(4.56)^{\frac{1}{2}} = 0.107]. \tag{88}$$

But, by Eqs. 56, 60, and 61, the 28 km/sec velocity of "ordinary meteoroids" corresponds to the mass of the same "ordinary meteoroids" by:

$$(v_a, m) = (28\,\text{km/sec}, 10^{(\log_{10} 28 - 1.51)(0.046)^{-1}} = 10^{-1.37}\ \text{gm}) . \tag{89}$$

Therefore, by Eqs. 88 and 89, the mass and density correspondence for ordinary meteors is:

$$(m, \rho) = (10^{-1.37}\,\text{gm}, 0.107 = 10^{-0.972}) . \tag{90}$$

Because meteoroid density varies with the square root of the meteor luminous efficiency factor, and mass varies directly with it, and if one will assume in the absence of more definitive information that, at any specified value of mass, the standard deviation of $\log_{10} \rho$ bears approximately the same relation to the standard deviation of $\log_{10} F_>$ as it would if all of the variances in them were due only to an uncertainty in the meteor luminous efficiency factor, then, by Eqs. 7, 37, 44, 48, 49, and 87,

$$\sigma_{y_4} = \sigma_{\log_{10} \rho} = |\beta_4|\,\sigma_{\log_{10} m} = |\beta_4/\beta_1|\,\sigma_{\log_{10} F_>} = |\beta_4/\beta_1|\,\sigma_{y_1} =$$
$$= |\sigma_{y_1}/\beta_1||\beta_4| = |1.10/-1.19||\beta_4| = 0.924\,|\beta_4| . \tag{91}$$

Estimates for values of density ρ to correspond with mass m for the micrometeoroids are not so firmly established as for ordinary meteoroids. Bjork [6] says: "It is reasonable to expect that the smaller meteoroids will not have the lacy, porous structure needed to give a specific gravity of 0.05, but that their density will increase as one goes down the mass scale, eventually approaching the [2.8] specific gravity of stone, the basic component, as very small sizes are reached." For the density of particles of 7μ radius, Alexander, McCracken, and LaGow [1] assumed 1.4×10^{-9} gm, saying: "The value 1 gm cm^{-3} for mass density is somewhat higher than the value 0.05 gm cm^{-3} used by Whipple. The value used by Whipple is probably much more appropriate to the photographic meteors, for which it was determined, than for the dust particles in the direct measurements range of sizes." But Whipple [41] cautions: "We have no sound basis upon which to assume densities for smaller than ordinary meteor particles, except for the effect of light pressure or other physical effects..." However Öpik's [43] analysis, as discussed

in Section III.B.1., leads to Eq. 54, which the author prefers to accept also for the purpose of the present report. Then as Eq. 87 is that of a line with two points given by Eqs. 54 and 90,

$$\beta_4 = -0.079 \tag{92}$$

$$\overline{y}_4 = -1.08. \tag{93}$$

Then also, by Eqs. 91 and 92,

$$\sigma_{y_4} = 0.073. \tag{94}$$

These Eqs. 92 through 94 results for β_4, $\overline{y}_4$, and σ_{y_4} respectively when used in Eq. 87 together with the Eq. 29 criteria for contours of equi-probable values of ρ versus m, seem very well to represent the avialable information when the mass m is in the vicinity of that ($10^{-1.37}$ gm) for "ordinary meteoroids"; and the 50% confidence contour seems appropriate over the entire interval $10^{-10} < m < 10^{1}$ gm. But the 25 and 75% confidence contours must diverge more for small values of m because of the greater uncertainty. Therefore, Eq. 87 will be replaced by the following more flexible model:

$$\log_{10} \rho = y_5 (\log_{10} m - \beta_5) + y_4 + \beta_4 \beta_5 \tag{95}$$

where: (1) β_4, $\overline{y}_4$, and σ_{y_4} are as before, with the values given in Eqs. 92 through 94 respectively, (2) β_5 is the constant common logarithm of the Eq. 90 mass of the "ordinary meteoroids"

$$\beta_5 = -1.37 \tag{96}$$

and (3) y_5 is an approximately normally distributed random variable, statistically independent of y_4, with standard deviation σ_{y_5} and mean $\overline{y}_5$. The latter is, by Eqs. 87, 92, and 95,

$$\overline{y}_5 = \beta_4 = -0.079 \quad . \tag{97}$$

Then by Eqs. 29 and 95 through 97, the 50% confidence contour of ρ versus m is invariant with respect to replacing Eq. 87 with Eq. 95.

The σ_{y_5} standard deviation will be so chosen that the above estimate by Alexander, McCracken, and LaGow [1], which can be represented by

$$(\rho, m) = (1, 1.4 \times 10^{-9} = 10^{-8.85} \text{ gm}), \tag{98}$$

is on the 75% confidence contour; i.e., on the contour of values which have a 25% chance of being less than ρ. Therefore, with Eqs. 7, 29, and 95 through 98,

$$\sigma_{y_5} = 0.075 \ . \tag{99}$$

By applying the Eqs. 7 and 29 criteria and the Eqs. 92 through 94, 96, 97, and 99 numerical values to Eq. 95 one gets the contours of equi-probable values of ρ versus m which are illustrated graphically in Fig. 4. The results seem to be satisfactory throughout the interval $10^{-10} < m < 10^{1}$ gm.

D. METEOROID DAMAGE

1. Nature and Function of Material Versus Effects. The meteoroid hazard to space vehicles, or the damage to be expected from meteors, is put in appropriate perspective by the following statement by Rinehart [34] about the concept of quality of failure: "In any particular target, the failure will usually be a complex of many qualities of failure, although frequently a single quality predominates. The basic problems to consider are what qualities of failure prevail in the situa- at hand, which ones are of interest, and whether each quality of failure is an energy-absorbing process, a momentum-absorbing process, or a combination of both. And lastly, what is the quantitative relationship between the extent of failure of a particular quality and the energy and momentum available to cause the failure?... a few overall qualities of failure are the following: perforation or puncture, volume of crater, volume of failed region, scabbing, spallation, and amount of abrasion..."

The quality of failure which will be emphasized in this report is failure by puncture of an empty metallic single shell. This has been necessary to keep the problem from getting too far afield. Should it be expected that the same shell would be more easily punctured when filled with a liquid? Or is it just the other way around? And then, of course, one would want to know what temperature, pressure,

shock wave, etc., the liquid is subjected to in the temporal vicinity, what chemical reaction follows, and is there an explosive vaporization which further rends the structure? But such comprehensive considerations are beyond the scope of this report.

2. Crater Volume in Thick Targets Versus Energy and Momentum for Meteoroids at Normal Incidence. Rinehart [34] illustrates his contention that the volume of the crater produced in a target material by an impacting meteoroid is a linear combination of the kinetic energy ($\frac{1}{2} mv_c^2$) and momentum (mv_c) of the meteoroid with respect to the target. He says that: "...if a failure results from application of an impulse under which the material dislodges easily and offers the inertia of its own mass as a resistance to motion, then the process is a momentum transfer (a flicking away of material, so to speak). On the other hand, if the body steadily continues to resist application of the force, the process is energy-absorbing (pushing of material against a force). Perforation of a thin plate by a projectile, or penetration into a laminated structure such as wood, are momentum-absorbing processes. An energy-absorbing process is the formation of a deep crater in steel by the impact of a heavy projectile. In most real materials, the failure will be a combination of the two."

Both Eichelberger [17] and Beard [3] imply that, for any given target and meteoroid material and structure, crater volume is essentially proportional to kinetic energy ($\frac{1}{2} mv^2$) independently of momentum (mv). Eichelberger [17], says: "The [empirical] results support very strongly the conclusion from fundamental considerations that cavitation plays the dominant role in crater formation in ductile materials and explains the linear relationship between volume and energy." Beard [3], says: "It is most probable that energy considerations of evaporation, rather than momentum effects, dominate the surface interaction of the micrometeorites with a satellite."

3. Crater Depth in Thick Targets Versus Energy, Momentum, and Density of Meteoroids. Typically the various empirical and theoretical formulas for meteoroid crater depth [e.g., 48] are the product of the cube root of crater volume and the following three factors: (1) the crater-shape factor, (2) the plate-thickness factor, and (3) the angle-of-incidence factor. Thus, crater depth p_0 is proportional to the 1/3 power of the mass m if crater volume is a linear combination of energy ($\frac{1}{2} mv_c^2$) and momentum (mv_c). Since Bjork [6] indicates that p_0 is proportional to $(mv_c)^{1/3}$ he is therefore presumably implying that

crater volume is proportional to momentum (mv) independently of energy ($\frac{1}{2} mv^2$).

An example of a penetration law that does not infer that crater volume is a linear combination of energy and momentum, is the law that can be deduced from data which is graphically presented by Hoenig and Ritter [25]; i.e., that the logarithm of penetration depth is linearly related to the logarithm of crater diameter in the same interval of kinetic energy over which they indicate with another graph that crater diameter is proportional to the square root of kinetic energy. In other words, crater depth p_0 is proportional to $m^{\frac{1}{2}} v_c$ for the experiments performed by Partridge at the University of Utah with wax pellets where impact velocity exceeds the velocity of sound in the target material.

But to what must one say that the crater depth is proportional, when so many factors are available from which to choose? Interestingly enough the geometric mean of Hoeing and Ritter's [25] factor $m^{1/2} v_c$, and Bjork's [6] factor, $(mv_c)^{1/3}$ is $(m^{5/4} v_c^2)^{1/3}$, which is very close to Eichelberger's factor, $(mv_c^2)^{1/3}$. However, the author feels that neither momentum nor kinetic energy should be inconsequential. He prefers, in the absence of more convincing contrary information, to consider that crater depth, at normal incidence and for given target and meteoroid material and shape, is represented by

$$p_0 \sim m^{\beta_6} v_c^{y_6} \tag{100}$$

where: (1) β_6 is a constant which will be assumed to have the same value,

$$\beta_6 = 1/3 \tag{101}$$

as when crater volume is a linear combination of momentum and energy, and (2) y_6 is an approximately normally distributed random variable, which represents both randomness and uncertainty due to insufficient information. The algebraic mean for y_6 is considered to be the exponent of the geometric mean of the factors, $v_c^{1/3}$ and $v_c^{2/3}$, which would represent proportionality of crater volume to momentum and energy, respectively, i.e.,

$$\bar{y}_6 = 1/2 \ . \tag{102}$$

The standard deviation for y_6 is considered to be one third of the difference between the above mentioned exponents 2/3 and 1/3, i.e., $1/3 \leq y_6 \leq 2/3$ at approximately 87% confidence:

$$\sigma_{y_6} = 1/9 \tag{103}$$

Herrmann and Jones [48] say: "Data on cratering has been reported by Summers for copper projectiles impacting copper targets at 7,000 and 11,000 ft/sec [2.13 and 3.35 km/sec], and by Kineke for steel discs impacting lead targets at 16,400 ft/sec [5.00 km/sec]. Both experiments noted that the data for oblique impact compared very well with that for normal impact, if penetration versus the normal component of velocity is plotted." This result can be represented by

$$v_{x_2} = v_c \cos x_2 \tag{104}$$

where x_2 is the angle of incidence relative to the normal to the target surface and is therefore a random variable. Presumably this relation, Eq. 104, will also be sufficiently appropriate for meteoroids hitting other metal targets. By Eq. 104 the angle-of-incidence factor by which the right side of Eq. 100 must be multiplied is $(\cos x_2)^{y_6}$, and therefore Eq. 100 is replaced by

$$p_0 \sim m^{1/3} (v_c \cos x_2)^{y_6} \ . \tag{105}$$

To establish the statistical definition of x_2 in Eq. 105, consider a meteoroid incident on a sphere and an axis parallel to the path of the meteoroid but containing the center of the sphere. The plane normal to the axis and containing the center of the sphere divides the sphere into two hemispheres, and the one which is hit is orthogonally projected onto its base plane. If x_2 is the angle of incidence of the meteoroid relative to the normal to the surface of the hemisphere, then all meteoroids which are parallel to the axis and which will have angles in the interval between x_2 and $x_2 + dx_2$ will be projected onto a ring with radii in the interval between $R \sin x_2$ and $R \sin x_2 + d(R \sin x_2)$. The relative area of the differential ring is the probability density function for angular incidence x_2, i.e.,

$$f(x_2) = |\sin 2x_2| \ . \tag{106}$$

Since $f(x_2)$ by Eq. 106 is symmetric with respect to $\frac{1}{4}\pi$, it follows that both the mean and median of x_2 are given by

$$\bar{x}_2 = \tfrac{1}{4}\pi \text{ radians} . \tag{107}$$

Then, by substituting the Eqs. 106 and 107 expressions into Eq. 5, one finds that the standard deviation of x_2 is

$$\sigma_{x_2} = (\pi^2/16 - \tfrac{1}{2})^{\frac{1}{2}} = 0.34 \text{ radians}. \tag{108}$$

Herrmann and Jones' [48] survey and analysis of published theoretical and empirical results for the crater depth in thick metal plates by hypervelocity projectiles are believed to provide a sufficient basis for establishing the crater shape factor. They conclude that, above a velocity transition region which depends on the target and projectile densities, the projectile strength does not affect penetration, particularly for ductile projectiles, and: "If this is true, then the only factor to account for differences in penetration in a given target material by different projectile materials is the projectile density." By an analysis of the empirical results published for many different target and projectile materials, Herrmann and Jones [48] developed the following empirical non-dimensional penetration law:

$$p_0/d = (0.36 \pm 0.07)(\rho_p/\rho_t)^{2/3}(\rho_p v_c^{\,2}/H_t)^{1/3} \tag{109}$$

where: (1) H_t is the Brinell Hardness of the target, (2) ρ_p and ρ_t are the projectile and target densities respectively, and (3) d is the diameter of the projectile. The velocity exponent in Eq. 109 will agree with that in Eq. 100 when the last term in Eq. 109 is raised to the $3y_6/2$ power, then Eq. 109 can be replaced by

$$p_0/d = 10^{y_7}(\rho_p/\rho_t)^{2/3}(\rho_t v_c^{\,2}/H_t)^{\frac{1}{2}y_6} \tag{110}$$

where y_7 is an approximately normally distributed random variable, indicating the uncertainty in the relation and in the information about it, determined by:

$$10^{y_7} = 0.36 \pm 0.07 = \bar{x}_3 \pm \sigma_{x_3} \tag{111}$$

where one assumes from various comments that the numerically indicated uncertainty is standard deviation rather than probable error or mean deviation (mean absolute error). Also, Herrmann and Jones [48] have explained that they got the results, Eqs. 109 and 111, by plotting

and fitting on log-log paper. So it is evident that x_3 in Eqs. 109 and 111 is actually the antilogarithm of the more basic random variable y_7. Because it is subject to the normal law of error more directly in the fitting process than is x_3, y_7 can more appropriately be considered as approximately normally distributed. Presumably y_7 can be considered to have mean $\overline{y}_7$ and standard deviation σ_{y_7} given by:

$$\overline{y}_7 = \log_{10} 0.36 = -0.44 \tag{112}$$

$$\sigma_{y_7} = \log_{10} (0.36 + 0.07) - \log_{10} 0.36 = 0.08 \tag{113}$$

But, when the units for ρ_t are gm/cm^3 and those for v_c are km/sec, then a further proportionality constant is necessary in the last term in Eqs. 109 and 110 because, by the definition in the Metals Handbook [50] the units for Brinell Hardness H_t are kilograms of force per square millimeter, i.e., Eq. 110 must be replaced by

$$p_0/d = 10^{y_7} (\rho_p/\rho_t)^{2/3} (k\rho_t v_c^2/H_t)^{\frac{1}{2}y_6} \tag{114}$$

where

$$k = \frac{(gm/cm^3)(10^5\ cm/sec)^2}{(980,665\ gm\ cm/sec^2)/(10^{-1}\ cm)^2} = 102\ . \tag{115}$$

Let both p and d in Eq. 114 be measured in centimeters. Then, assuming that meteoroid hazard is not essentially misrepresented by a spherical meteoroid of mass m grams.

$$d = 2(3m/4\pi\rho_p)^{1/3}\ . \tag{116}$$

Herrmann and Jones [48] make the following further comment about Eq. 109: "It might be noted that a slightly higher exponent in ρ_t might be expected to fit slightly better. However, it was decided to retain the advantages of a non-dimensional fit. Small changes ($\pm$ 10%) in exponents of the non-dimensional parameters did not significantly alter the mean deviation." But because, by Eq. 102, $\overline{y}_6$ is $\frac{1}{2}$, the mean effect on ρ_t of having adjusted the exponent of v_c to y_6 is that the exponent of ρ_t has been lowered. Also, the value to be used for the exponent of (ρ_p/ρ_t) is uncertain, to a considerable extent, as is well illustrated by Bjork [6]. Therefore, an approximately normally distributed random variable exponent y_8 will be introduced with mean $\overline{y}_8$, which is related to $\overline{y}_6$ in that it restores the mean value

of the exponent, and with standard deviation σ_{y_8} indicative of a probable error which is 10% of the mean; i.e.,

$$-\bar{y}_8 + \tfrac{1}{2}\bar{y}_6 = -2/3 + 1/3$$

$$\bar{y}_8 = \tfrac{1}{2}\bar{y}_6 + 1/3 = 7/12 = 0.583 \tag{117}$$

$$\sigma_{y_8} = 0.10(7/12)/0.6745 = 0.086 \tag{118}$$

Therefore, by replacing the exponent of the density ratio in Eq. 114 by y_8, by substituting the Eq. 115 value for k in Eq. 114, by multiplying the resulting equation by Eq. 116, and by multiplying the right side of the resulting equation by the angle-of-incidence factor $(\cos x_2)^{y_6}$ as in Eq. 105, one still gets the somewhat biased formula for the thick-target crater depth p_0 due to a spherical meteoroid:

$$p_0 = 10^{y_7}(102)^{\frac{1}{2}y_6}(2)(3/4\pi)^{1/3}\rho_t^{\frac{1}{2}y_6 - y_8} H_t^{-\frac{1}{2}y_6}\rho_p^{y_8 - 1/3} m^{1/3}(v_c \cos x_2)^{y_6} \tag{119}$$

when the following units are used: p_0, cm; ρ_t and ρ_p, gm cm^{-3}; H_t, Brinell Hardness Number; m, gm; v_c, km sec^{-1}; and x_2, radians.

Equation 119 is still biased because the slope of $\log_{10} p_0$ versus $\log_{10} v_c$ has been changed; but the intercept still has to be adjusted so that the combined effect of a change in slope and in intercept will be that some favored point is invariant. Eq. 119 is based on Eq. 109, which is based on the upper segments of broken linear fits to data points in the $\log_{10}(p/d)$ versus $\log_{10} v_c$ domain, for various projectile and target materials including hard aluminum alloys, and for $\log_{10} v_c$ typically in an interval of roughly $\log_{10}$ 3 km/sec $< \log_{10} v_c < \log_{10}$ 5 km/sec. Then take the favored point as

$$(\rho_p, \rho_t, H_t, v_c) = (2.80,\ 2.80,\ 135,\ 4)\ . \tag{120}$$

Then the factor 10^{y_9} by which one must multiply the right side of Eq. 119 to remove the bias is that which, at the Eq. 120 point, gives the following equality:

$$(\rho_p/\rho_t)^{y_8}\rho_p^{-1/3}(102\,\rho_t v_c^{\,2}/H_t)^{\frac{1}{2}y_6}10^{y_9} = (\rho_p/\rho_t)^{1/3}(102 v_c^{\,2}/H_t)^{1/3}\ . \tag{121}$$

Then by Eqs. 120 and 121, the factor 10^{y_9} is related to y_6 as follows:

$$10^{y_9} = \left[102\,(4)^2\,/135\right]^{1/3\,-\,\frac{1}{2}y_6}\,(2.80)^{1/3} \tag{122}$$

Therefore, the above-mentioned bias is removed by multiplying the right side of Eq. 119 by the right side of Eq. 122, getting:

$$p_0 = 4.01\,(10)^{y_7}(8.44\,\rho_t/H_t)^{\frac{1}{2}y_6}\rho_t^{\,-y_8}\rho_p^{\,y_8-1/3}\,m^{1/3}(v_c\cos x_2)^{y_6}\,. \tag{123}$$

It is of some interest to see how Eq. 123 compares with the following Eq. 124 for aluminum projectiles and thick aluminum targets reported by Bjork [6]:

$$p_0 = 1.09\,(mv_c)^{1/3} \tag{124}$$

where the units are as in Eqs. 119 through 123. Assuming relatively pure aluminum metal with the following density and Brinell Hardness Number:

$$(\rho_t,\ H_t) = (2.70,\ 23 < H_t < 44),\ \text{say}\ (2.70,\ 34) \tag{125}$$

then at normal incidence, with vanishing x_2, one can equate the right sides of Eqs. 123 and 124, substitute the mean values 0.50, -0.44, and 0.583 for $\overline{y}_6$, $\overline{y}_7$, and $\overline{y}_8$ from Eqs. 102, 112, and 117 respectively and solve for the value of v_c, i.e.,

$$v_c = 2.3\ \text{km/sec}\ . \tag{126}$$

Then the Eq. 123 formula gives values of thick-target crater depth larger than by the Eq. 124 formula by a factor $(v_c/2.3)^{1/6}$, which is

$$(6.3/2.3)^{1/6} = 1.18 \tag{127}$$

at the 6.3 km/sec value for v_c used in the experiments on which the Eq. 124 formula is based. This Eq. 127 result is well within the Eq. 111 indicated experimental accuracy; and one does not know for sure if the Brinell Hardness Number of the aluminum was as low as is assumed in Eq. 125. The Eq. 127 factor vanishes when H_t is increased to 66, or to some value less than 66 if the density is also increased. One will therefore decide that Eq. 123 is satisfactory for thick targets.

4. Thickness of a Just-Penetrable Shell Versus Mass, Density, Velocity, and Angle of Incidence of Meteoroids. The thickness p of a just-penetrable shell is related to the thick-target crater depth p_0 by the target thickness factor $10^{y_{10}}$, i.e.,

$$p/p_0 = 10^{y_{10}} \tag{128}$$

where y_{10} is an approximately normally distributed random variable which represents both the randomness of the process and the uncertainty in the information about it. Bjork's comment is: "The calculations were made for thick targets, but enough information was obtained to deduce that if a projectile penetrates a depth p in a thick target, it will just penetrate a sheet of the same target material which is 1.5p thick." Black [49] says: "To allow a 'bulge' although 'just not perforated', a skin gage of 1.5 times crater depth is generally assumed. (Note that this should be 2 - 3 if the results of Jaffe and Rittenhouse are used.)" Eichelberger's [17] "rule of thumb" is that: "...a meteoroid... will produce a hemispherical crater of volume τ... If the thickness of the skin is less than $(3\tau/2\pi)^{1/3}$ (or even if it is slightly greater), the skin will be perforated." In other words, the factor is $2^{1/3} = 1.26$ or slightly greater. Herrmann and Jones [48] illustrate experimental results (which they attribute to Kinard et.al. at NASA Langley) and an empirical formula indicating that, as shell thickness is decreased toward the value p, the value of p/p_0 approaches:

$$p/p_0 \rightarrow (1/1.3)^2 + 1 = 1.59 \tag{129}$$

These Eq. 129 results are said to have been obtained with "...steel and aluminum projectiles into aluminum targets at impact velocities between 5,000 and 13,000 ft/sec" ... i.e., between 1.5 and 4 km/sec. When C is the confidence that this Eq. 128 factor is equal to or less than the stated value, then it seems appropriate that the above-mentioned four estimates should be accepted as follows:

$$(C,\ 10^{y_{10}}) = (0.16,\ 1.26),\ (0.41,\ 1.50),\ (0.50,\ 1.59),\ (0.976,\ 2.5) \tag{130}$$

$$\overline{y}_{10} = 0.20 \tag{131}$$

$$\sigma_{y_{10}} = 0.10. \tag{132}$$

SECTION IV. DESIGN AND OPERATIONAL PARAMETERS

A. JUST-PENETRABLE METEOROID MASS VERSUS THICKNESS, DENSITY, AND HARDNESS OF THE FREE-WALL OF A SPACE VEHICLE IN A NEAR EARTH-ORBIT

By taking the logarithm of the product of Eqs. 123 and 128 and substituting the Eqs. 62 and 95 expressions for $\log_{10} v_c$ and $\log_{10} \rho_p$ one finds

$$\begin{aligned}\log_{10} p = {} & \log_{10} 4.01 + y_{10} + y_7 + \tfrac{1}{2} y_6 \log_{10} 8.44 + \tfrac{1}{2} y_6 \log_{10} (\rho_t / H_t) - \\ & - y_8 \log_{10} \rho_t + y_6 \log_{10} (\cos x_2) + y_3 y_6 + \\ & + (y_8 - 1/3) \left[y_4 + \beta_5 (\beta_4 - y_5) \right] + \left[(1 - y_5)/3 + \right. \\ & \left. + y_5 y_8 + \beta_3 y_6 \right] \log_{10} m \end{aligned} \tag{133}$$

With the values 0.041, -0.079, -1.37, $\frac{1}{4}\pi$, 1.52, -1.08, -0.079, $\frac{1}{2}$, -0.44, 0.538, and 0.20 for β_3, β_4, β_5, $\bar{x}_2$, $\bar{y}_3$, $\bar{y}_4$, $\bar{y}_5$, $\bar{y}_6$, $\bar{y}_7$, $\bar{y}_8$, and $\bar{y}_{10}$ from Eqs. 83, 92, 96, 107, 84, 93, 97, 102, 112, 117, and 131 respectively, it follows by Eqs. 3 and 4 that the expected value of $\log_{10} p$ in Eq. 133 is:

$$E\left[\log_{10} p\right] = 1.06 - 0.29 \log_{10} \rho_t - 0.25 \log_{10} H_t + 0.338 \log_{10} m \, . \tag{134}$$

And with the further values 0.34, 0.17, 0.073, 0.075, 1/9, 0.08, 0.086, and 0.10 for σ_{x_2}, σ_{y_3}, σ_{y_4}, σ_{y_5}, σ_{y_6}, σ_{y_7}, σ_{y_8}, and $\sigma_{y_{10}}$ from Eqs. 108, 86, 94, 99, 103, 113, 118, and 132 respectively, it follows by Eq. 7 that the standard deviation of $\log_{10} p$ in Eq. 133 is:

$$\begin{aligned}\sigma_{\log_{10} p} = {} & \left\{ 0.053 + \left[0.204 + 0.056 \log_{10} (\rho_t / H_t) + 0.0046 \log_{10} m \right]^2 + \right. \\ & + \left[0.093 + 0.086 \log_{10} \rho_t + 0.0068 \log_{10} m \right]^2 + \\ & \left. + \left[0.021 + 0.015 \log_{10} m \right]^2 \right\}^{\frac{1}{2}} . \end{aligned} \tag{135}$$

These Eqs. 133 through 135 results are illustrated graphically in Figs. 5 and 6 for the following two respective metals:

$$(\rho_t, H_t) = (2.80, 135): \text{ hard aluminum alloy} \tag{136}$$

$$= (7.42, 310): \text{ Harder stainless steel} \tag{137}$$

and for the assumption that $\log_{10} p$ in Eq. 133 is sufficiently nearly normally distributed that the Eqs. 134 and 135 values for the mean and standard deviation can be used in the Eq. 29 formula relating confidence and values of the antilogarithm of an approximately normally distributed random variable.

B. METEOROID PUNCTURE-FLUX VERSUS THICKNESS, DENSITY, AND HARDNESS OF THE FREE (EMPTY) WALL OF A SPACE VEHICLE IN A NEAR-EARTH ORBIT

The penetration and/or puncture flux ϕ is that value of $F_>$ in Eq. 37 corresponding to a just-puncturable value of m. The following Eq. 138 formula for ϕ is found by solving Eq. 133 explicitly for $\log_{10} m$ and substituting the resulting expression into Eq. 37; i.e.,

$$\begin{aligned}\log_{10}\phi = y_1 + \beta_1 \Big\{ &\log_{10} p - \log_{10} 4.01 - y_{10} - y_7 - \tfrac{1}{2} y_6 \log_{10} 8.44 - \\ &- \tfrac{1}{2} y_6 \log_{10} (\rho_t / H_t) + y_8 \log_{10} \rho_t - y_6 \log_{10} (\cos x_2) - \\ &- y_3 y_6 - (y_8 - 1/3)\left[y_4 + \beta_5(\beta_4 - y_5)\right]\Big\} \left[(1 - y_5)/3 + y_5 y_8 + \beta_3 y_6\right]^{-1}.\end{aligned} \tag{138}$$

The random statistical variable ϕ, the puncture-flux is found, by taking the antilogarithm of Eq. 138, to be a function of nine statistically independent random variables (y_1, x_2, y_3 through y_8, and y_{10}), all of which are approximately normally distributed except x_2. If the right side of Eq. 138 were just a linear combination of these random variables and if x_2 were nearly normally distributed, then $\log_{10}\phi$ would also be a normal random variable, with mean given by using the means of the other random variables in Eq. 138, and Eq. 29 would be rigorously applicable for finding the contours of equi-probable values of ϕ as a function of p. The difference here is that the right side of Eq. 138 involves some products and ratios rather than just a linear combination of the random variables. But it will be assumed to be a sufficiently

accurate approximation here that $\log_{10}\phi$ is normally distributed with a mean value given by using the means of the other random variables in Eq. 138. Then, with the values -1.19 and -12.86 for β_1 and $\bar{y}_1$ from Eqs. 48 and 44 respectively, and with the other numerical values that were used in Eq. 133 to get Eq. 134, it follows from Eq. 138 that the mean or expected value of $\log_{10}\phi$ is:

$$E\left[\log_{10}\phi\right] = -9.13 - 3.52\log_{10} p - 1.01\log_{10}\rho_t - 0.881\log_{10} H_t. \tag{139}$$

And with the value 1.10 for σ_{y_1} from Eq. 49, and with the other numerical values that were used to get Eq. 135 from Eq. 133, it follows by Eq. 7 that the standard deviation of $\log_{10}\phi$ in Eq. 138 is:

$$\sigma_{\log_{10}\phi} = \left[\left(\frac{\partial \log_{10}\phi}{\partial y_1}\right)^2 \sigma_{y_1}^2 + \left(\frac{\partial \log_{10}\phi}{\partial x_2}\right)^2 \sigma_{x_2}^2 + \right.$$

$$\left. + \sum_{i=3}^{8}\left(\frac{\partial \log_{10}\phi}{\partial y_i}\right)^2 \sigma_{y_i}^2 + \left(\frac{\partial \log_{10}\phi}{\partial y_{10}}\right)^2 \sigma_{y_{10}}^2\right]^{\frac{1}{2}} \tag{140}$$

$$\left(\frac{\partial \log_{10}\phi}{\partial y_1}\right)^2 \sigma_{y_1}^2 = 1.21 \tag{141}$$

$$\left(\frac{\partial \log_{10}\phi}{\partial x_2}\right)^2 \sigma_{x_2}^2 = 0.36 \tag{142}$$

$$\left(\frac{\partial \log_{10}\phi}{\partial y_3}\right)^2 \sigma_{y_3}^2 = 0.090 \tag{143}$$

$$\left(\frac{\partial \log_{10}\phi}{\partial y_4}\right)^2 \sigma_{y_4}^2 = 0.0028 \tag{144}$$

$$\left(\frac{\partial \log_{10}\phi}{\partial y_7}\right)^2 \sigma_{y_7}^2 = 0.08 \tag{145}$$

$$\left(\frac{\partial \log_{10}\phi}{\partial y_{10}}\right)^2 \sigma_{y_{10}}^2 = 0.12 \tag{146}$$

$$\left(\frac{\partial \log_{10}\phi}{\partial y_5}\sigma_{y_5}\right)^2 = (0.161\log_{10} p - 0.0956 + 0.0460\log_{10}\rho_t +$$

$$+ 0.0401\log_{10} H_t)^2 \tag{147}$$

$$\left(\frac{\partial \log_{10}\phi}{\partial y_6}\sigma_{y_6}\right)^2 = (0.0474\log_{10} p + 0.666 + 0.111\log_{10}\rho_t - \\ - 0.0859\log_{10} H_t)^2 \quad (148)$$

$$\left(\frac{\partial \log_{10}\phi}{\partial y_8}\sigma_{y_8}\right)^2 = (-0.0709\log_{10} p - 0.252 - 0.323\log_{10}\rho_t - \\ - 0.0177\log_{10} H_t)^2 \quad (149)$$

These results, Eqs. 138 through 149, applied to each of the two metals described by Eqs. 136 and 137, lead to the following formulas, Eqs. 150 through 153, for the means and standard deviations of the common logarithms of the puncture-fluxes ϕ as a function of shell thickness p: (1) for the hard aluminum alloy,

$$E\left[\log_{10}\phi\right] = -3.52\log_{10} p - 11.46 \quad (150)$$

$$\sigma_{\log_{10}\phi} = \left[2.34 + 0.146\log_{10} p + 0.033(\log_{10} p)^2\right]^{\frac{1}{2}} \quad (151)$$

and (2) for the hard stainless steel,

$$E\left[\log_{10}\phi\right] = -3.52\log_{10} p - 12.20 \quad (152)$$

$$\sigma_{\log_{10}\phi} = \left[2.50 + 0.148\log_{10} p + 0.033(\log_{10} p)^2\right]^{\frac{1}{2}} \quad (153)$$

When these results, Eqs. 150 through 153, are substituted into the Eq. 29 formula, one gets the contours of equi-probable values of puncture-flux ϕ versus shell thickness p which are illustrated graphically in Figs. 7 and 8 for the hard aluminum alloy and hard stainless steel respectively.

C. THICKNESS OF A FREE WALL VERSUS THE PRODUCT OF EXPOSED HEMISPHERICAL AREA AND DURATION FOR GIVEN PROBABILITIES OF NO PUNCTURE OF A VEHICLE IN A NEAR-EARTH ORBIT

By substituting the Eq. 138 expression for $\log_{10}\phi$ in the common logarithm of the natural logarithm of Eq. 33 and solving the resulting equation explicitly for $\log_{10} p$, one gets

$$\log_{10} p = \beta_1^{-1}\left[(1 - y_5)/3 + y_5 y_8 + \beta_3 y_6\right]\left[-\log_{10} At + \log_{10}(-\log_e R) - y_1\right] +$$
$$+ \log_{10} 4.01 + y_{10} + y_7 + \tfrac{1}{2} y_6\left[\log_{10} 8.44 + \log_{10}(\rho_t/H_t)\right] -$$
$$- y_8 \log_{10} \rho_t + y_6 \log_{10} \cos x_2 + y_3 y_6 + (y_8 - 1/3)\left[y_4 +\right.$$
$$\left. + \beta_5(\beta_4 - y_5)\right]. \qquad (154)$$

Because $\log_{10} p$ involves no ratios of random variables, it follows by Eqs. 3 and 4 that $\log_{10} p$ in Eq. 154 should stand an even better chance of being approximately normally distributed than does $\log_{10}\phi$ in Eq. 138, discussed already in Section IV. B.; especially there is more reason for assuming that the mean of the function is the function of the means. It will therefore be assumed that Eq. 29 is a sufficiently approximate formula for obtaining the antilogarithm of Eq. 154 expression for $\log_{10} p$. Then, with the same numerical values as were used to get Eqs. 139 through 149 from Eq. 138, the mean and standard deviation of the common logarithm of the free wall thickness p centimers necessary to increase to R the probability of no meteoroid puncture of an exposed hemispherical area A square meters during an interval of t seconds in orbit near the earth are respectively:

$$E\left[\log_{10} p\right] = 0.284\left[\log_{10} At - \log_{10}(-\log_e R)\right] - 0.288 \log_{10} \rho_t -$$
$$- 0.25 \log_{10} H_t - 2.37 \qquad (155)$$

$$\sigma_{\log_{10} p} = \left[\left(\frac{\partial \log_{10} p}{\partial y_1}\sigma_{y_1}\right)^2 + \left(\frac{\partial \log_{10} p}{\partial x_2}\sigma_{x_2}\right)^2 + \right.$$
$$\left. + \sum_{i=3}^{8}\left(\frac{\partial \log_{10} p}{\partial y_i}\sigma_{y_i}\right)^2 + \left(\frac{\partial \log_{10} p}{\partial y_{10}}\sigma_{y_{10}}\right)^2\right]^{\frac{1}{2}} \qquad (156)$$

$$\left(\frac{\partial \log_{10} p}{\partial y_1}\sigma_{y_1}\right)^2 = 0.0974 \qquad (157)$$

$$\left(\frac{\partial \log_{10} p}{\partial x_2}\sigma_{x_2}\right)^2 = 0.0289 \qquad (158)$$

$$\left(\frac{\partial \log_{10} p}{\partial y_3}\sigma_{y_3}\right)^2 = 0.0072 \qquad (159)$$

$$\left(\frac{\partial \log_{10} p}{\partial y_4}\sigma_{y_4}\right)^2 = 0.0002 \tag{160}$$

$$\left(\frac{\partial \log_{10} p}{\partial y_7}\sigma_{y_7}\right)^2 = 0.0064 \tag{161}$$

$$\left(\frac{\partial \log_{10} p}{\partial y_{10}}\sigma_{y_{10}}\right)^2 = 0.0100 \tag{162}$$

$$\left(\frac{\partial \log_{10} p}{\partial y_5}\sigma_{y_5}\right)^2 = \left[0.0129 \log_{10} At - 0.0129 \log_{10}(-\log_e R) - 0.145\right]^2 \tag{163}$$

$$\left(\frac{\partial \log_{10} p}{\partial y_6}\sigma_{y_6}\right)^2 = \left[0.00382 \log_{10} At - 0.00382 \log_{10}(-\log_e R) + 0.0556 \log_{10}(\rho_t/H_t) + 0.198\right]^2 \tag{164}$$

$$\left(\frac{\partial \log_{10} p}{\partial y_8}\sigma_{y_8}\right)^2 = \left[0.0057 \log_{10} At - 0.0057 \log_{10}(-\log_e R) + 0.086 \log_{10} \rho_t + 0.0196\right]^2. \tag{165}$$

These results, Eqs. 154 through 165, applied to each of the two metals described by Eqs. 136 and 137, lead to the following Eqs. 166 through 169 for formulas for the means and standard deviations of the common logarithms of the necessary free wall thickness p centimeters: (1) for the hard aluminum alloy,

$$E\left[\log_{10} p\right] = 0.284\left[\log_{10} At - \log_{10}(-\log_e R)\right] - 3.03 \tag{166}$$

$$\sigma_{\log_{10} p} = \left\{0.185 - 0.00229\left[\log_{10} At - \log_{10}(-\log_e R)\right] + 0.000213\left[\log_{10} At - \log_{10}(-\log_e R)\right]^2\right\}^{\frac{1}{2}} \tag{167}$$

and (2) for the hard stainless steel,

$$E\left[\log_{10} p\right] = 0.284\left[\log_{10} At - \log_{10}(-\log_e R)\right] - 3.24 \tag{168}$$

$$\sigma_{\log_{10} p} = \left\{0.192 - 0.00183\left[\log_{10} At - \log_{10}(-\log_e R)\right] + 0.000213\left[\log_{10} At - \log_{10}(-\log_e R)\right]^2\right\}^{\frac{1}{2}}. \tag{169}$$

When these results, Eqs. 166 through 169, are substituted into the Eq. 29 formula, one gets the contours of equi-probable values

of necessary equivalent free wall thickness p versus the effective area-time exposure product At as illustrated graphically in Figs. 9 through 11 for the hard aluminum alloy and values of 0.85, 0.90, and 0.95 respectively for the puncture-free probability R, and in Figs. 12 through 14 for the hard stainless steel and values of 0.85, 0.90, and 0.95 respectively for R.

D. VARIATION OF OPERATIONAL PARAMETERS

As an illustrative example, consider that one has a vehicle with a total surface area of 390 square meters (4200 square feet) of 0.318 cm (eighth-inch) free wall of hard aluminum alloy, and one wants to know how long the vehicle can remain in a near-earth orbit with not less than an even chance that the no-puncture probability is as high as 0.90.

In Fig. 10, the horizontal line at 0.318 cm, corresponding to the eighth-inch wall thickness, intersects the 50% confidence contour at the indicated ordinate, corresponding to the $10^{7.90}$ square-meter-seconds value for At. As the numerical values for meteoroid flux, which were established in Section III.A.4. and used in the derivation of the relations which are illustrated in Fig. 10, are based on the assumption that only half of the surface area of the vehicle which is facing away from the earth will be considered in the flux-area-time product, the appropriate value for A in this example is 195 square meters, corresponding to the 2100 square feet hemispherical area. The permissible exposure time is therefore ($10^{7.90}$/195) seconds, which is 4.8 days.

E. VARIATION OF DESIGN PARAMETERS

As a further illustrative example, consider that one has a vehicle with a total surface area of 390 square meters (4200 square feet), and one wants to know what equivalent free wall thickness of hard aluminum alloy will give not less than an even chance that the probability of no puncture is not less than 0.90 as the vehicle remains in a near-earth orbit for not less than 30 days. The (390)(30) square meter days corresponds to the $10^{8.70}$ square-meter-seconds value for At, for which an ordinate has been marked on Fig. 10. This ordinate crosses the 50% confidence contour at the 0.54 cm value for p, corresponding to the 0.21 inch neccessary wall thickness.

F. RELATIVE CONTRIBUTIONS TO THE DEGRADATION OF CONFIDENCE

One coincidental but convenient relation between wall thickness and confidence can be seen to be common to all of the Figs. 9 through 14: with both materials for all three values of the no-penetration probability, and for all values of the exposure product within the interval $10^{-1} \leq At \leq 10^{12}$ square meter seconds, confidence is increased from the 25% value to the 50% value, or from the 50% value to the 75% value, accurately by doubling the wall thickness.

The relative contributions to the uncertainty can best be taken as the relative components of the variance of the logarithm of the necessary wall thickness, i.e., by the ratios of each of Eqs. 157 through 165 to the square of Eq. 156. The numerical values, which are indicated in Table I, have been calculated for the specific example described in Section IV.E.

TABLE I

Parameter	Source of the Uncertainty	Magnitude of the Uncertainty
y_1	Flux versus Mass	53.2%
x_2	Angular Deviation from the Normal	15.8
y_3	Closing Velocity	3.9
y_4	Mass-Dependence of Density	0.1
y_5	Mass-Dependence of Density	0.2
y_6	Penetration Exponent of Velocity	10.8
y_7	Penetration Coefficient	3.5
y_8	Penetration versus Target Density	7.0
y_{10}	Target Thickness Factor	5.5

The last four lines in Table I indicate the relative components (of the variance of the logarithm of the necessary wall thickness) which are due to our inability to predict more accurately what will happen in a specified hypervelocity impact; and the sum total of these four components is only 26.8%. But if these four components could be entirely eliminated, then the probable error in the logarithm of the necessary wall thickness would only be reduced to 85.6% of its present value; i.e., $(1.000 - 0.268)^{\frac{1}{2}} = 0.856$.

G. AMELIORATING CONSIDERATIONS

Lest one might be apprehensive of the considerable free wall thicknesses which are inferred in Figs. 5 through 14, it is appropriate to note that Nysmith and Summers [33] report: "...two-sheet structures are probably the most efficient multiple-sheet structures. The most substantial gain in penetration resistance is achieved by filling the void between the sheets with a glass-wool filler. For the one case, investigated, namely, a two-sheet structure with a sheet spacing of one inch, the penetration resistance of the structure with the glass-wool filler is about twice as great as that of the structure without the filler material and about 4.4 times greater than that of a single sheet of material of the same total-sheet thickness."

SECTION V. CONCLUSIONS

It can be seen from the numerical results, which are graphically illustrated in Figs. 5 through 14, that if a vehicle which is very large, and which also has thin walls, remains very long in orbit near the earth, it may be punctured by a meteoroid.

For a vehicle of given size, given time in orbit, and given no-puncture probability, it is necessary to increase the effective free-wall thickness by a factor of 2.00 to change the confidence from 50% to 75%. If hypervelocity puncture effects on given materials were completely predictable for projectiles of specified density and velocity, then the above factor would be 1.81 instead of 2.00. This would help appreciably, but not so much as would a reduction in the uncertainty of the mean-time-between-hits per unit of surface area for meteoroids of mass equal to or greater than stated values.

The reader should be aware that there still exists some controversy over the available meteoroid flux, density, velocity and angular distribution statistics. Therefore, for any design studies the latest accepted values should be employed.

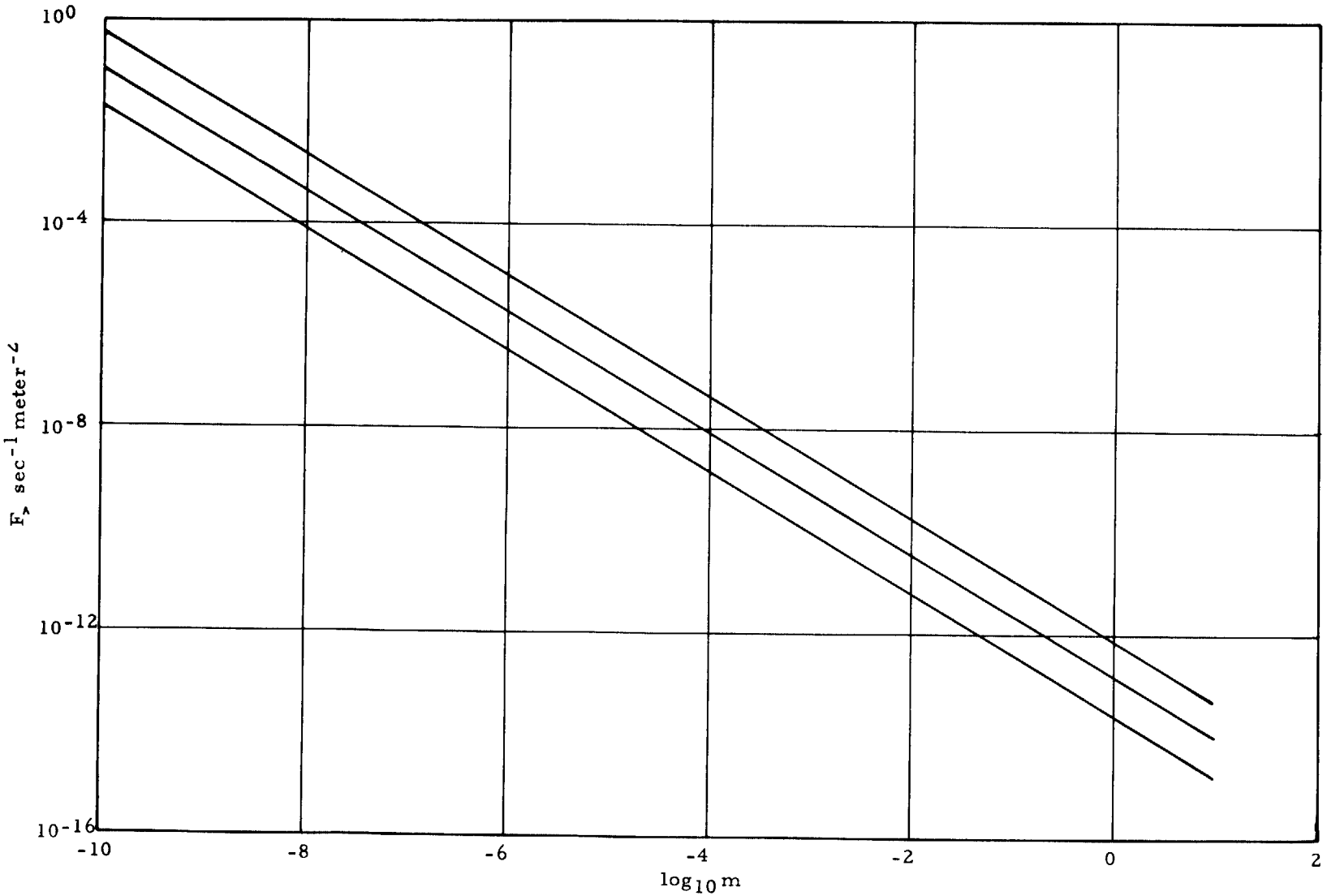

FIG. 1. MASS DEPENDENCE OF THE FLUX OF METEOROIDS ON A SPHERICAL SURFACE IN A NEAR EARTH ORBIT. MASS $\geq$ m (gm). AVERAGE NUMBER PER SECOND PER SQUARE METER AT 25, 50, AND 75% CONFIDENCE.

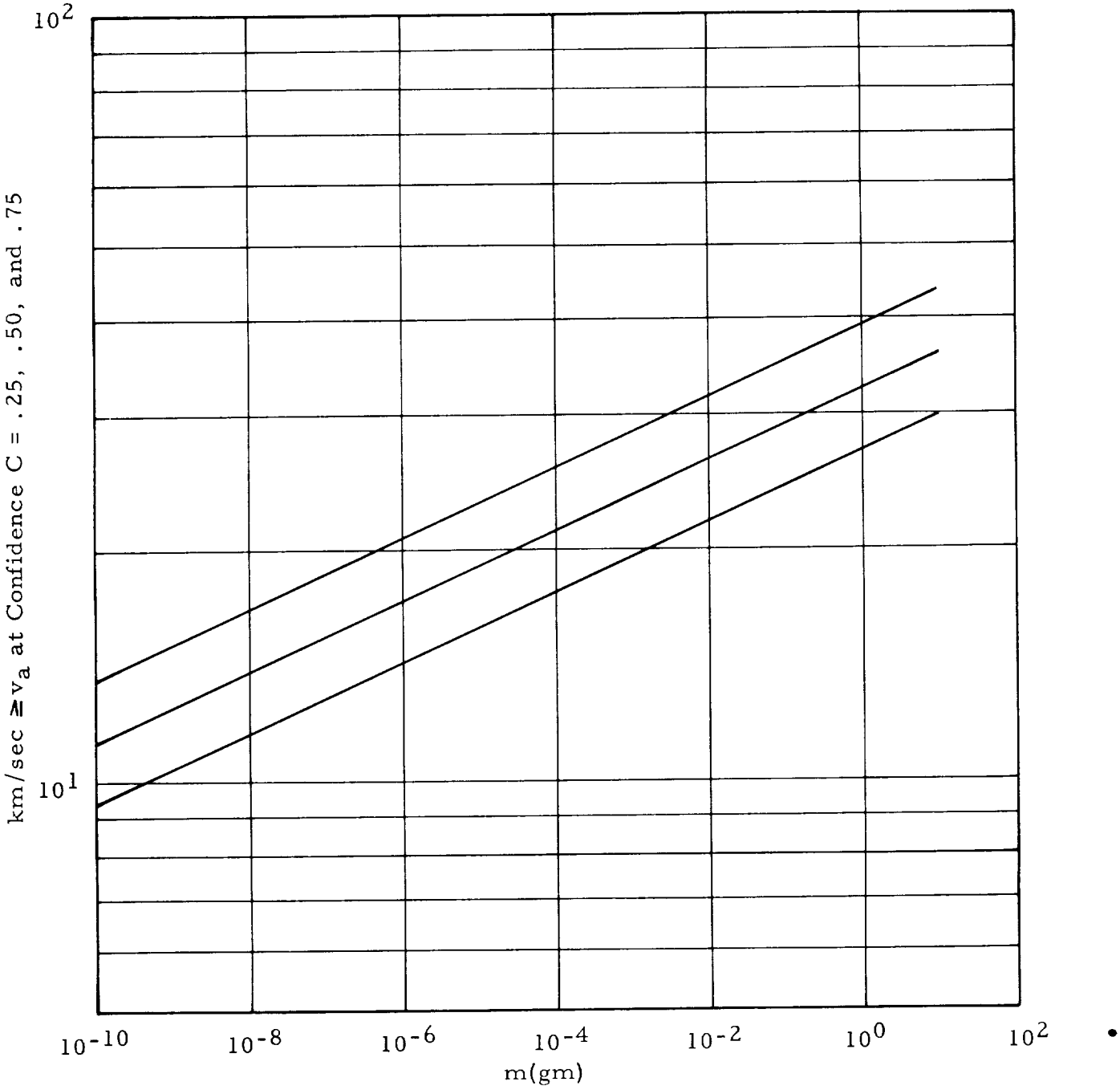

FIG. 2. MASS DEPENDENCE OF METEOROID VELOCITY RELATIVE TO THE EARTH'S ATMOSPHERE

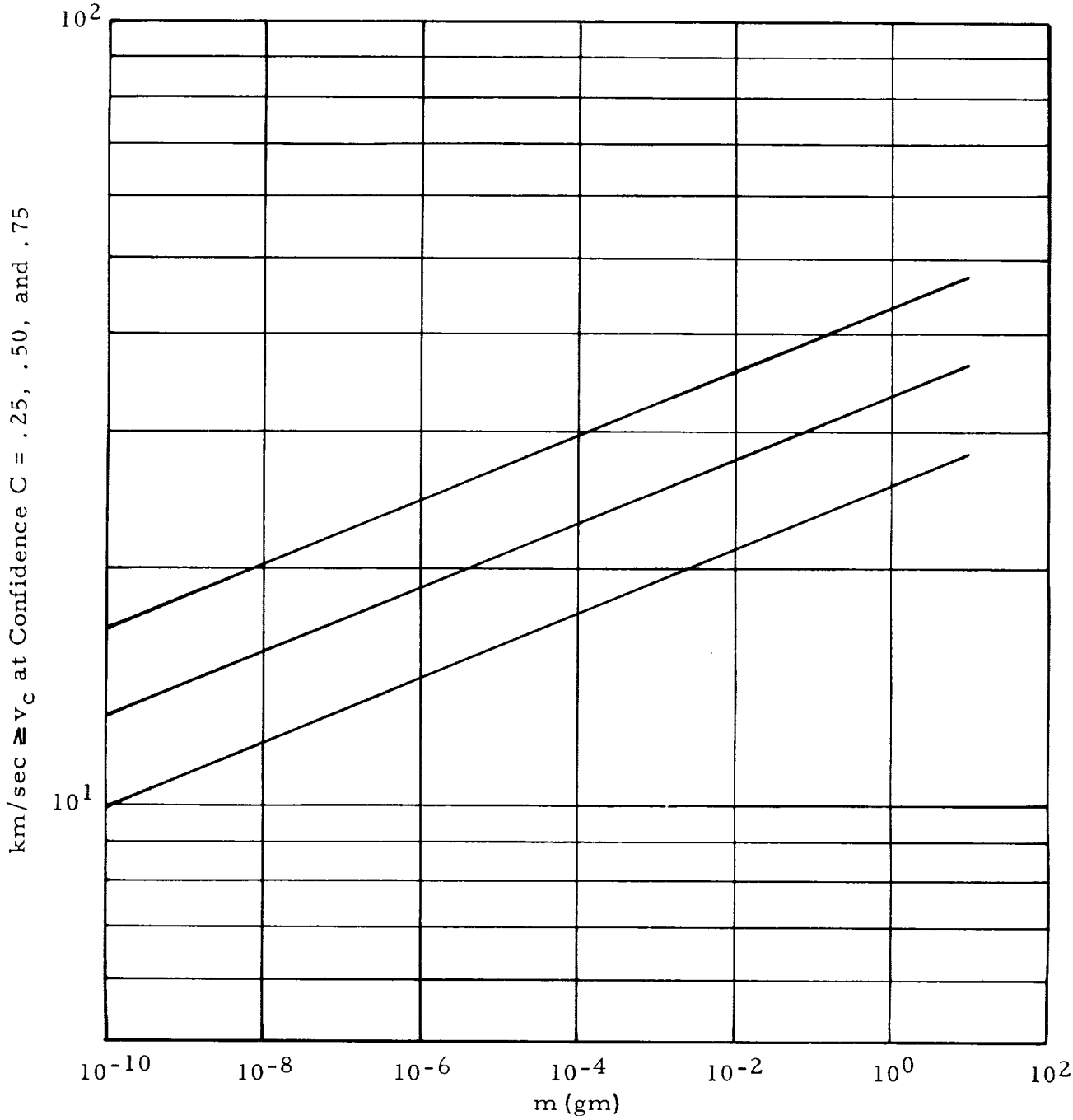

FIG. 3. MASS DEPENDENCE OF METEOROID VELOCITY RELATIVE TO A VEHICLE IN A NEAR-EARTH ORBIT

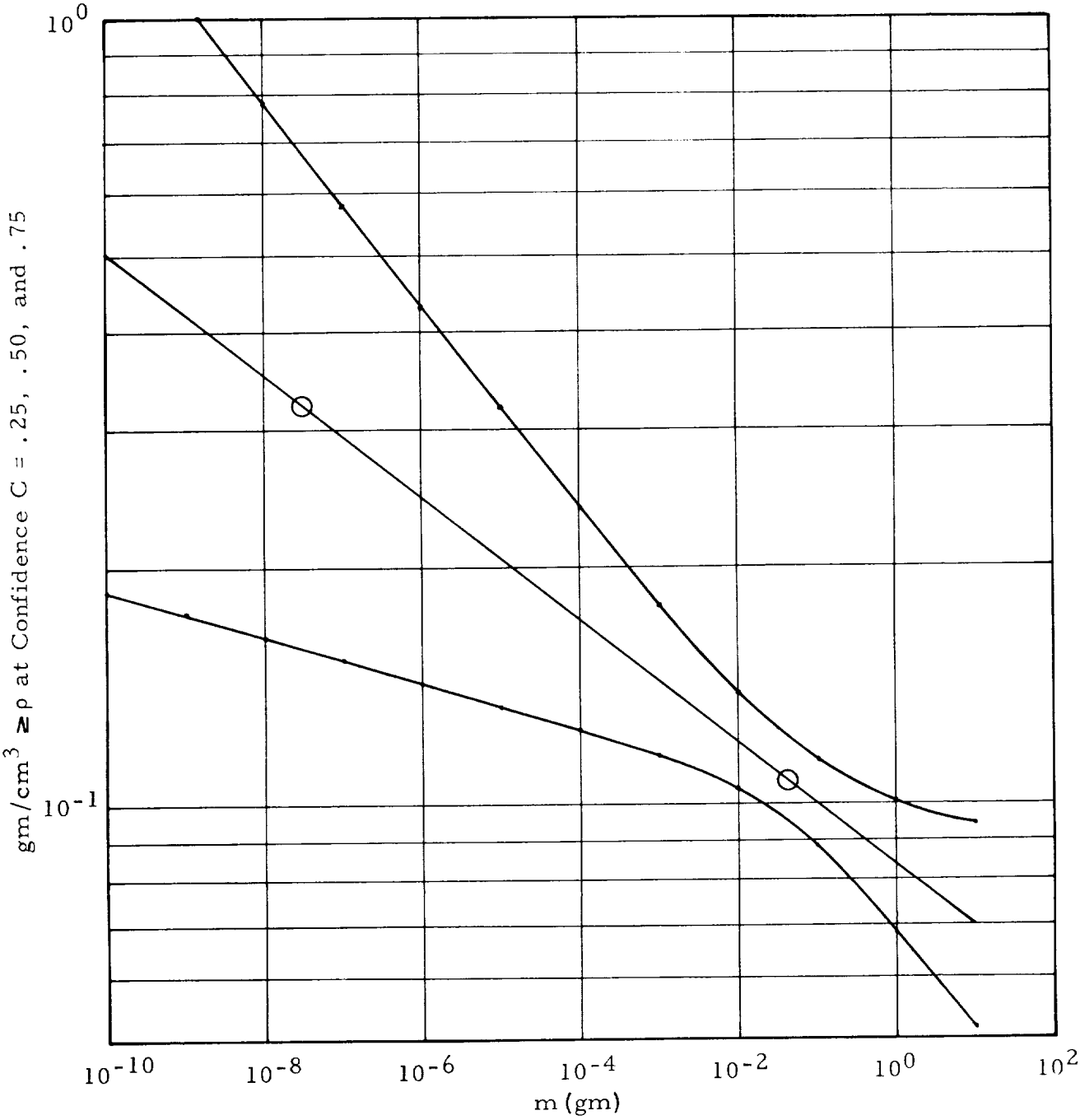

FIG. 4. MASS DEPENDENCE OF METEOROID DENSITY

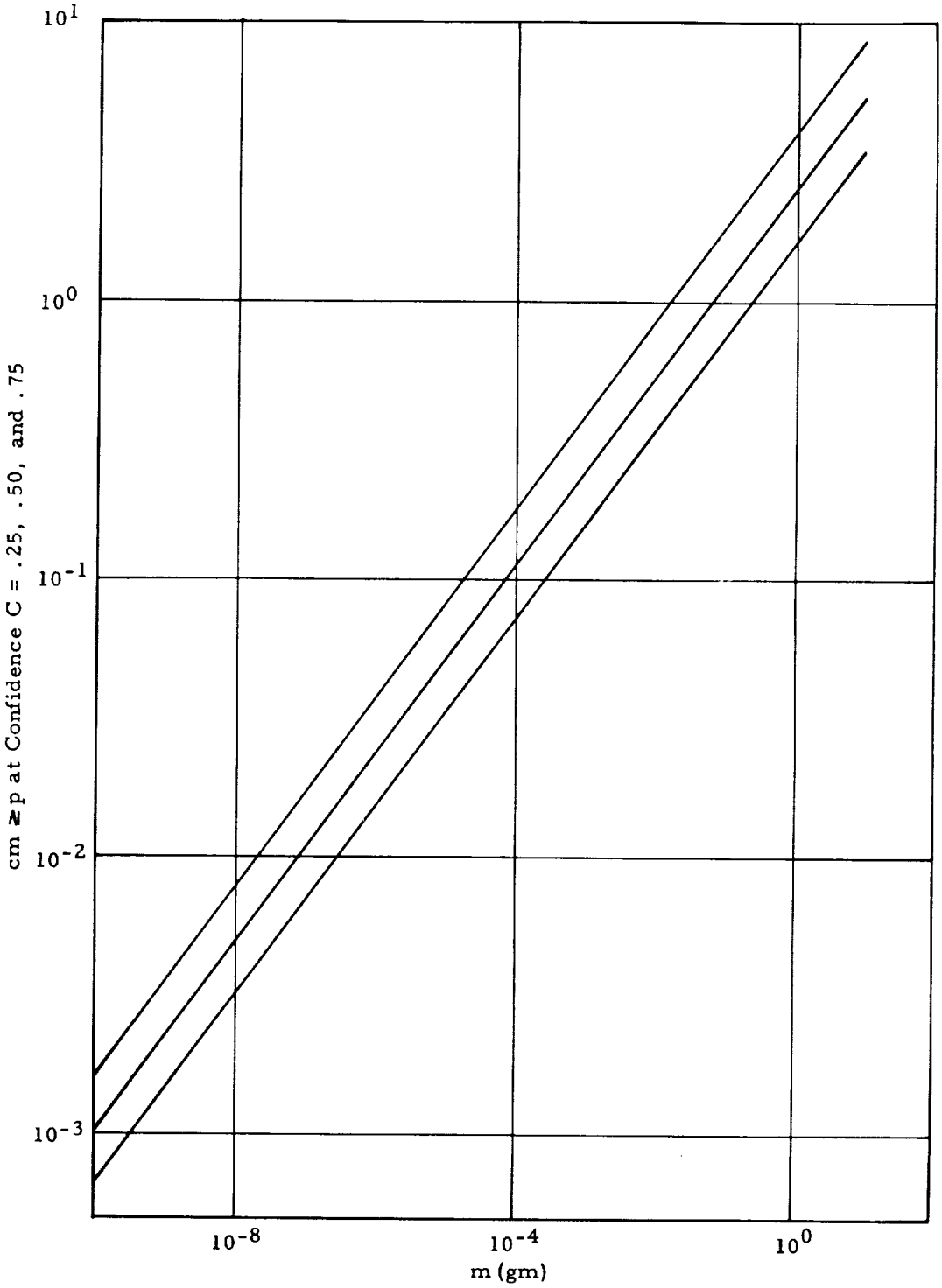

FIG. 5. MASS DEPENDENCE OF THE THICKNESS OF AN EMPTY SHELL OF HARD ALUMINUM ALLOY JUST PUNCTURABLE BY A METEOROID OF MASS m

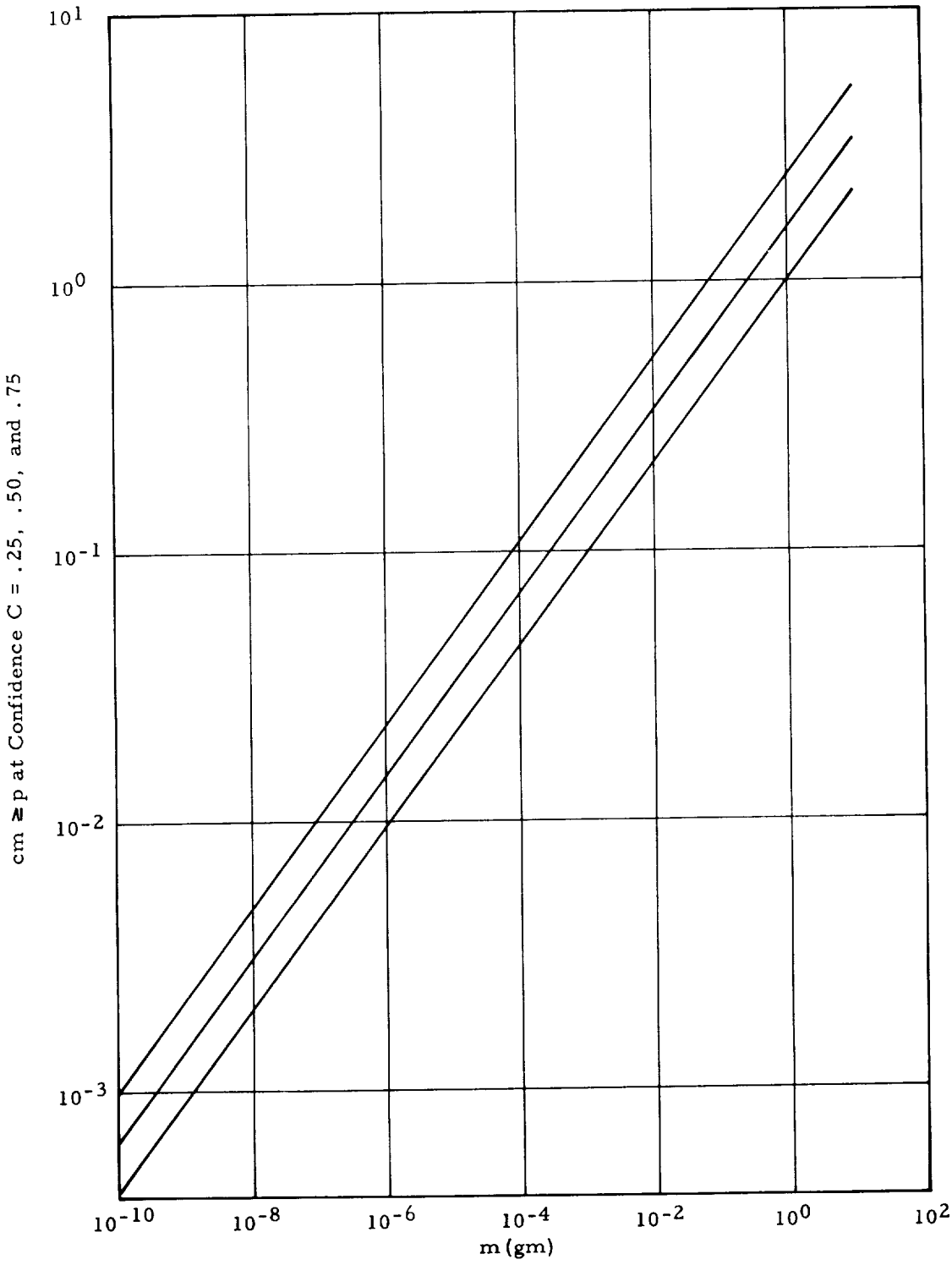

FIG. 6. MASS DEPENDENCE OF THE THICKNESS OF AN EMPTY SHELL OF HARD STAINLESS STEEL JUST PUNCTURABLE BY A METEOROID OF MASS m

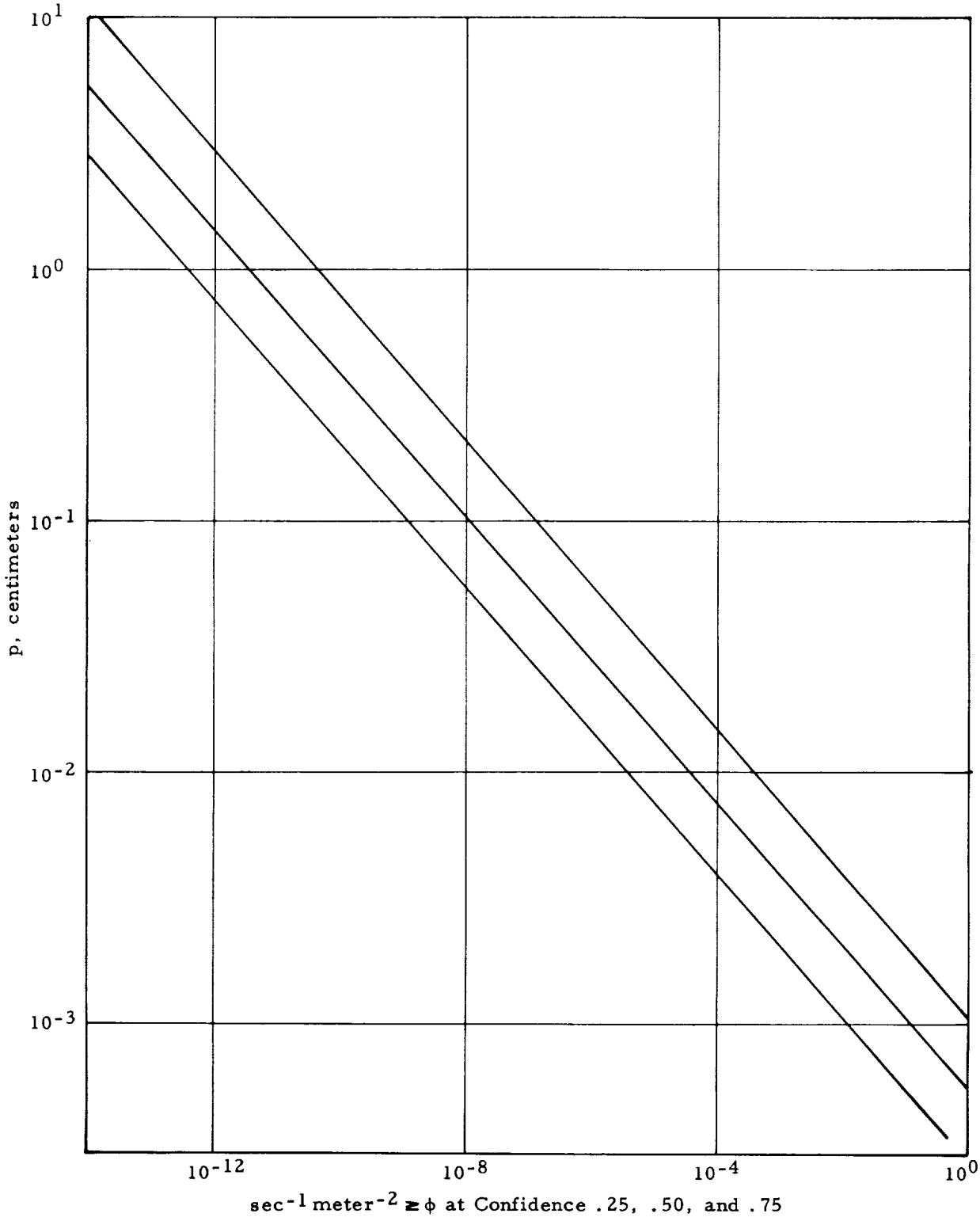

FIG. 7. METEOROID PUNCTURE FLUX FOR A FREE WALL OF HARD ALUMINUM ALLOY FOR A VEHICLE IN A NEAR-EARTH ORBIT

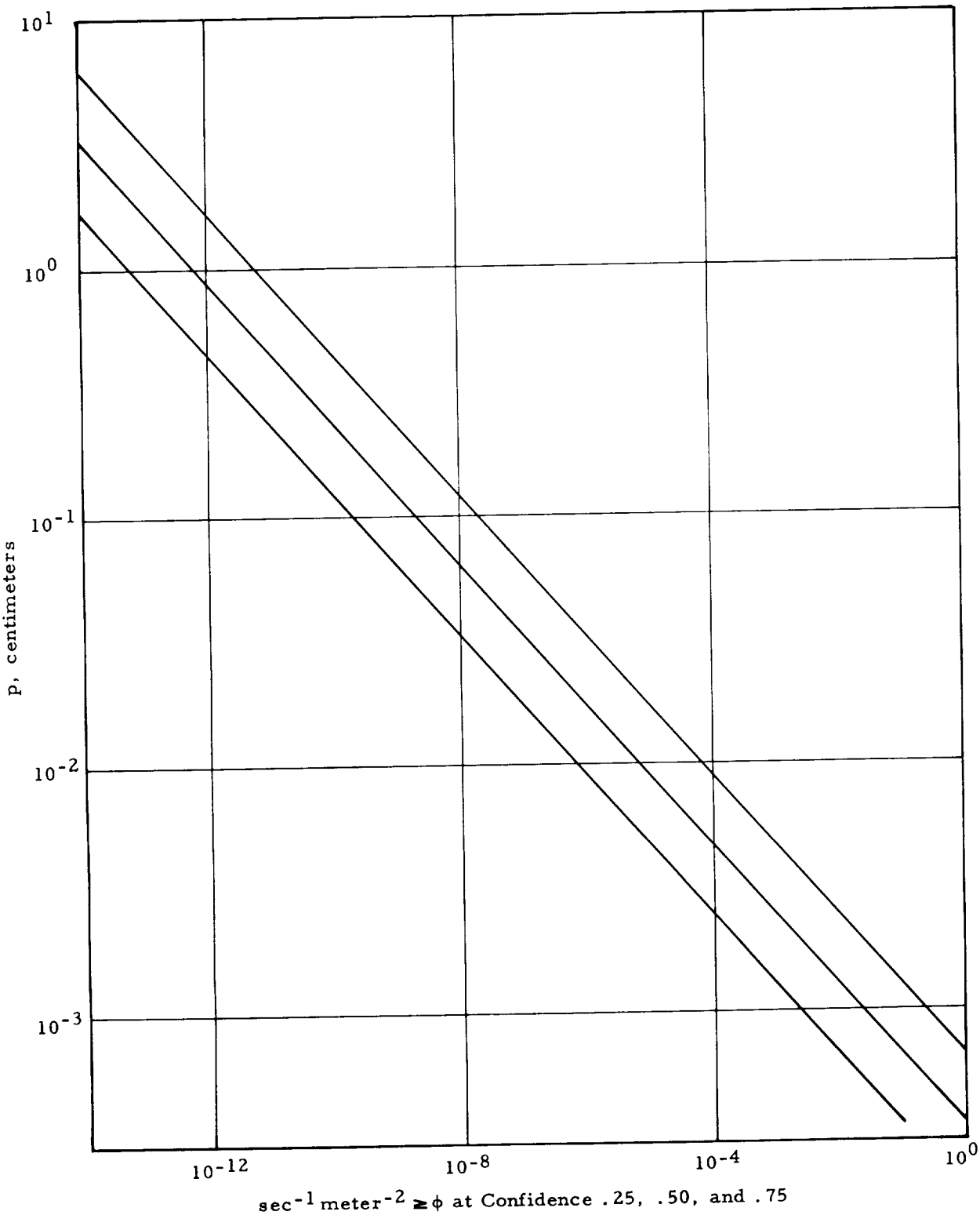

FIG. 8. METEOROID PUNCTURE FLUX FOR A FREE WALL OF HARD STAINLESS STEEL FOR A VEHICLE IN A NEAR-EARTH ORBIT

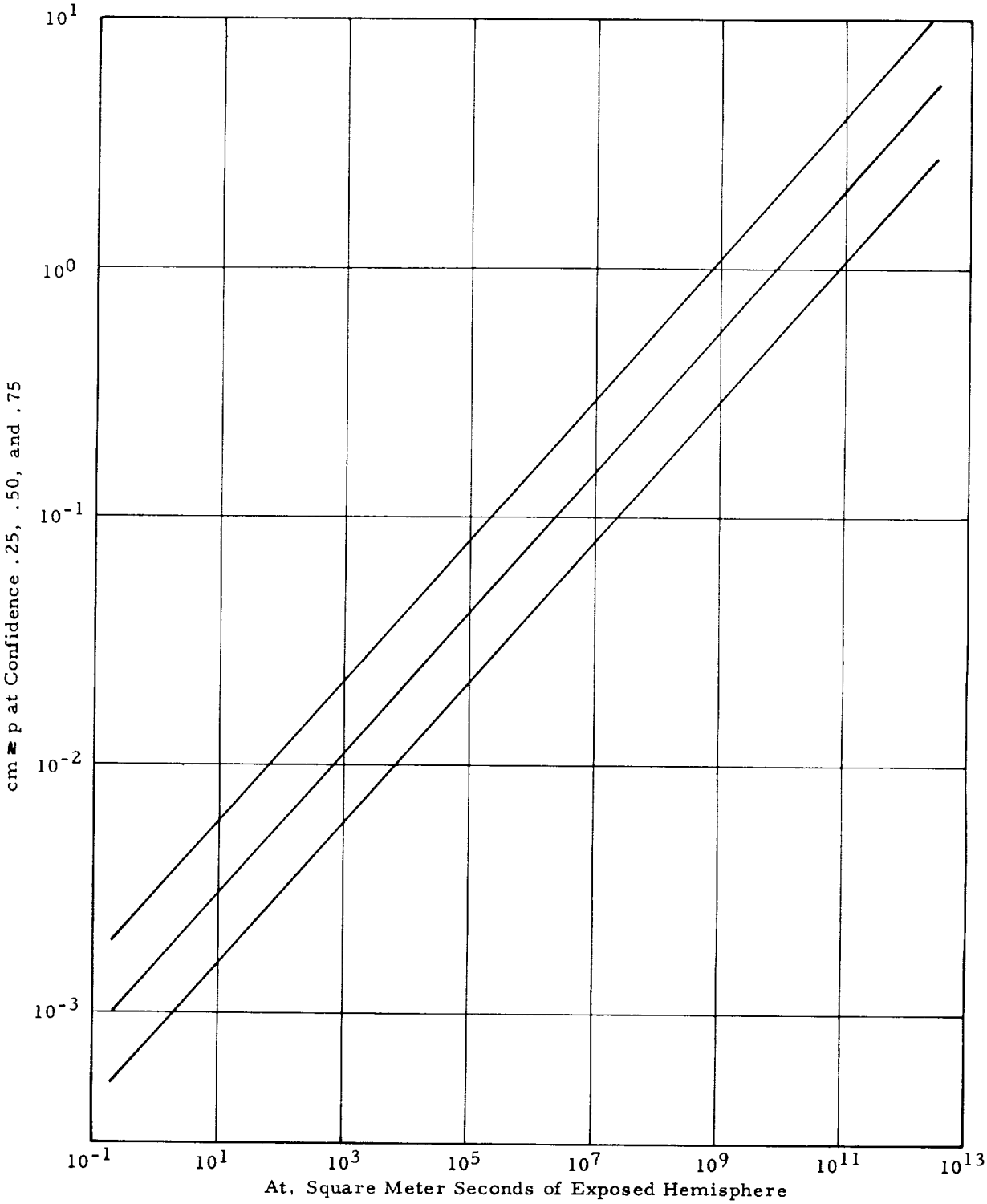

FIG. 9. NECESSARY THICKNESS OF HARD ALUMINUM ALLOY FOR .85 PROBABILITY OF NO PUNCTURE OF A SPHERICAL VEHICLE IN A NEAR-EARTH ORBIT VERSUS EXPOSURE At

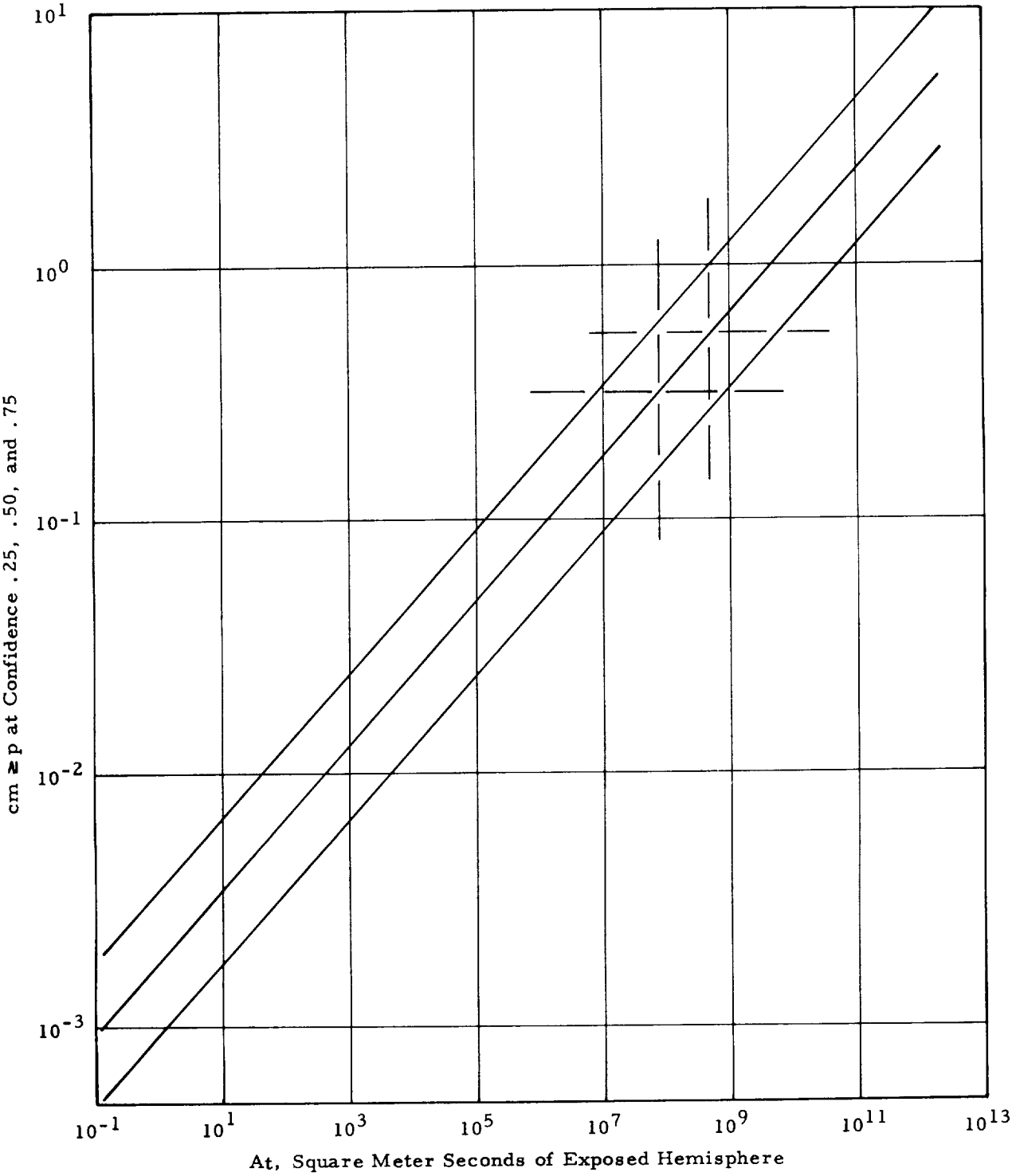

FIG. 10. NECESSARY THICKNESS OF HARD ALUMINUM ALLOY FOR .90 PROBABILITY OF NO PENETRATION OF A SPHERICAL VEHICLE IN A NEAR-EARTH ORBIT VERSUS EXPOSURE At

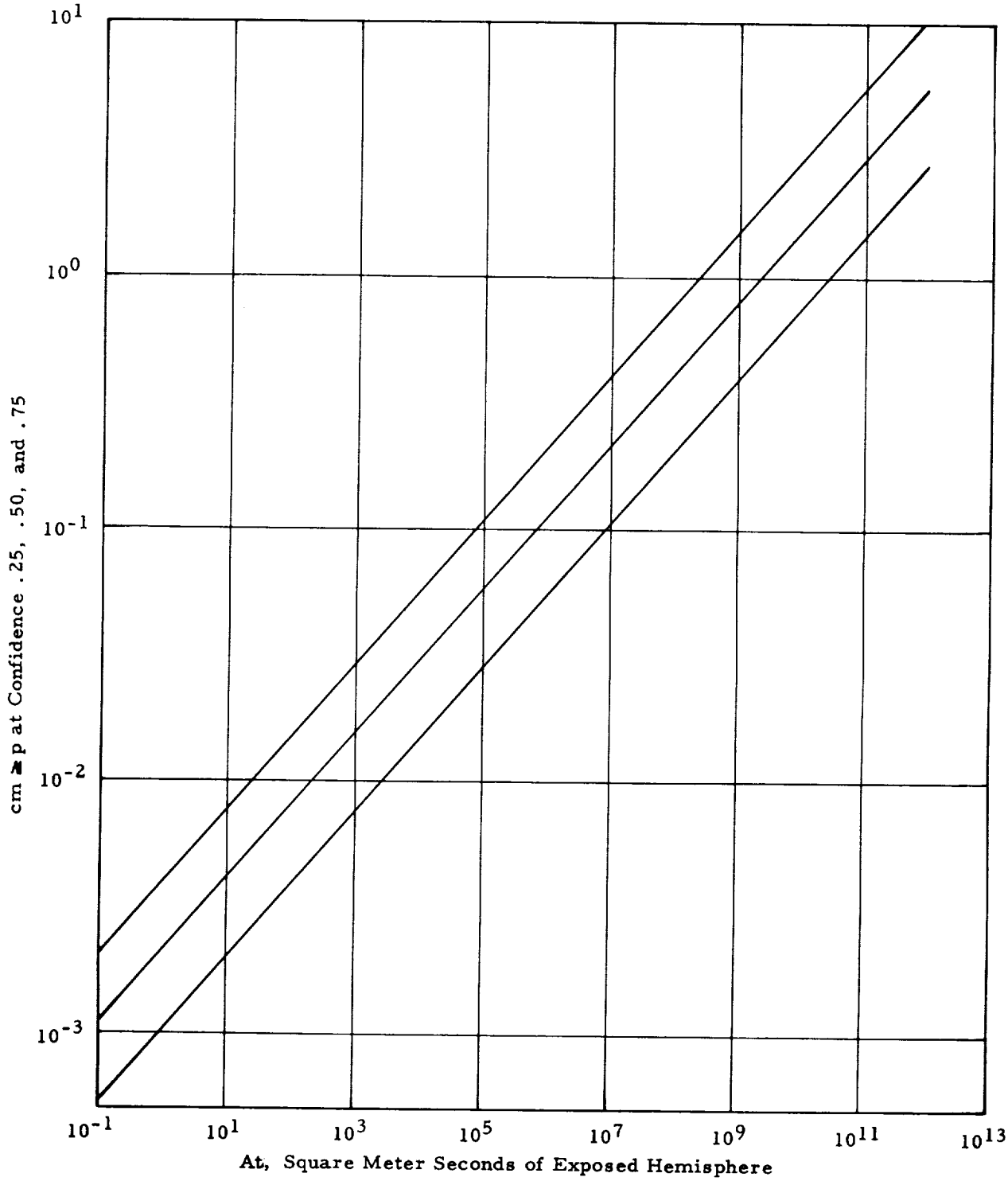

FIG. 11. NECESSARY THICKNESS OF HARD ALUMINUM ALLOY FOR .95 PROBABILITY OF NO PUNCTURE OF A SPHERICAL VEHICLE IN A NEAR EARTH ORBIT VERSUS EXPOSURE At

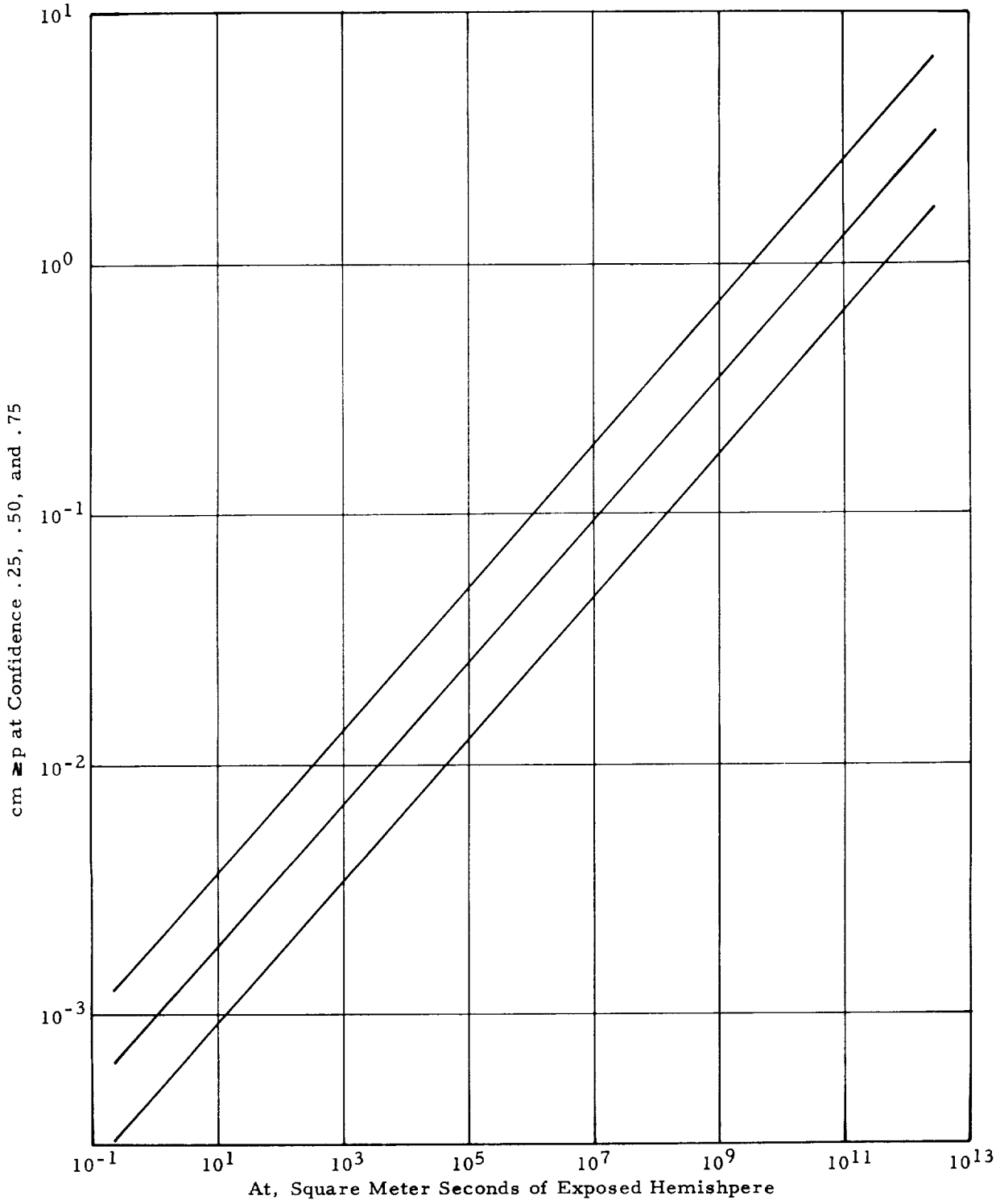

FIG. 12. NECESSARY THICKNESS OF HARD STAINLESS STEEL FOR .85 PROBABILITY OF NO PUNCTURE OF A SPHERICAL VEHICLE IN A NEAR-EARTH ORBIT VERSUS EXPOSURE At

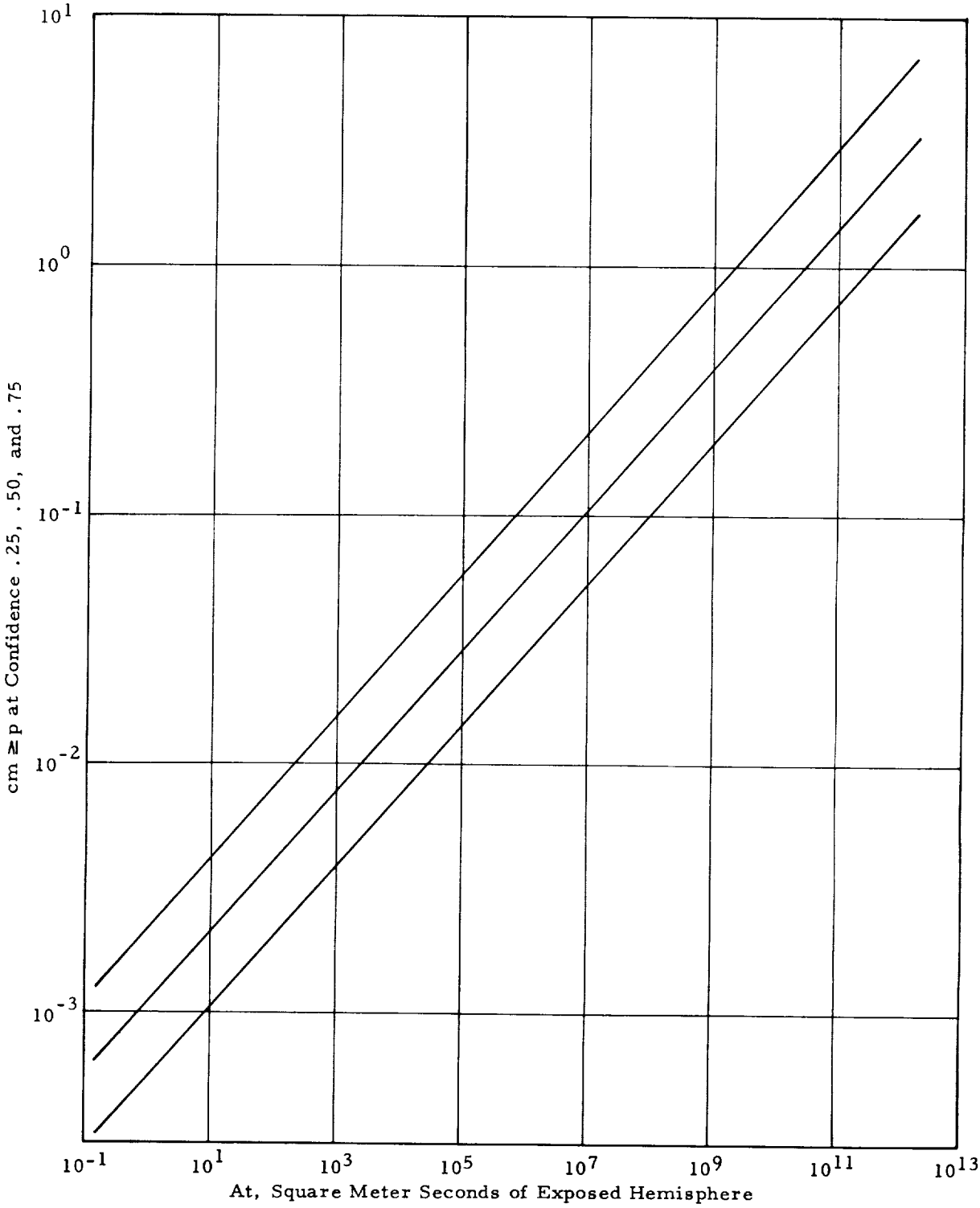

FIG. 13. NECESSARY THICKNESS OF HARD STAINLESS STEEL FOR .90 PROBABILITY OF NO PUNCTURE OF A SPHERICAL VEHICLE IN A NEAR-EARTH ORBIT VERSUS EXPOSURE At

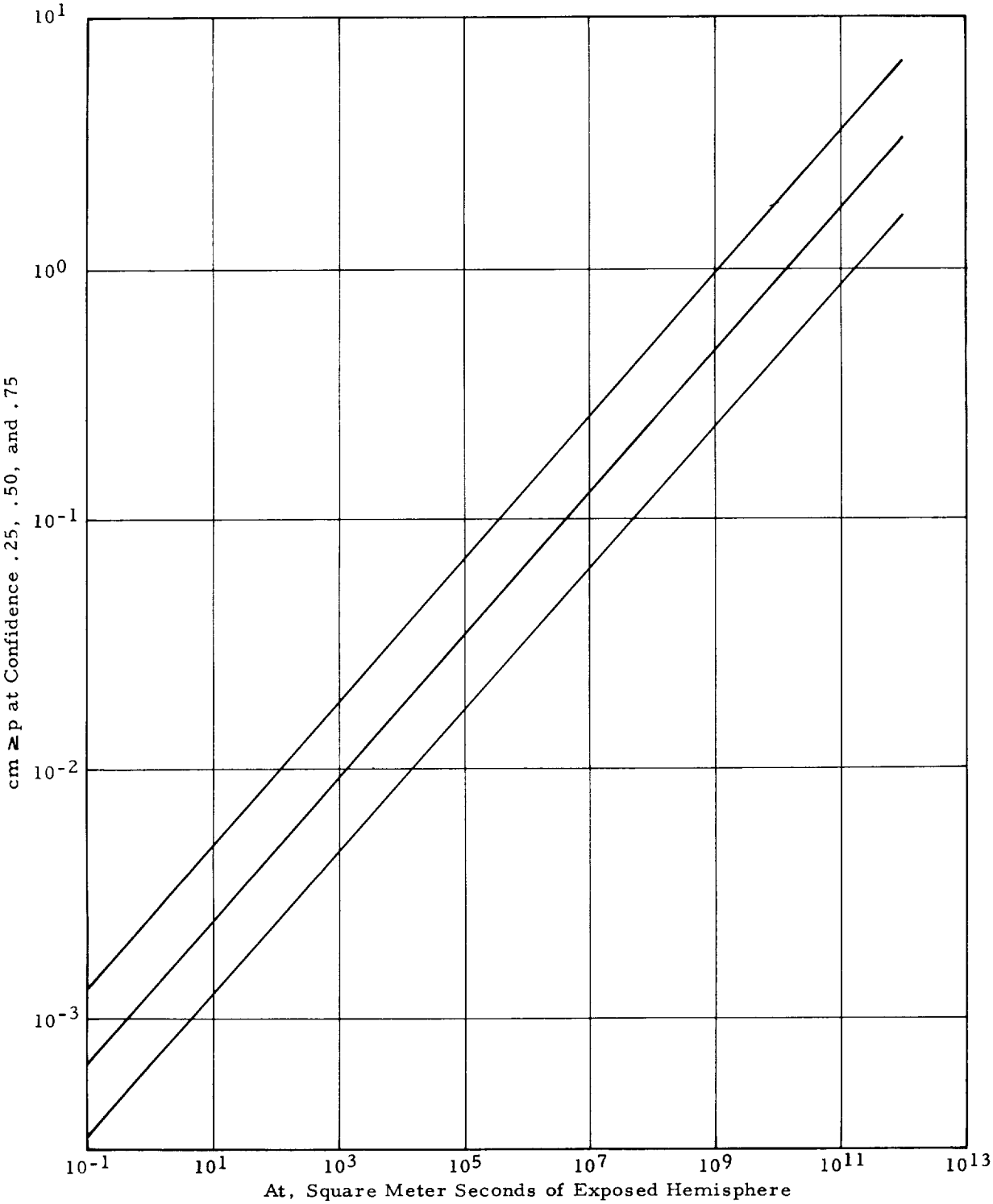

FIG. 14. NECESSARY THICKNESS OF HARD STAINLESS STEEL FOR .95 PROBABILITY OF NO PUNCTURE OF A SPHERICAL VEHICLE IN A NEAR-EARTH ORBIT VERSUS EXPOSURE At

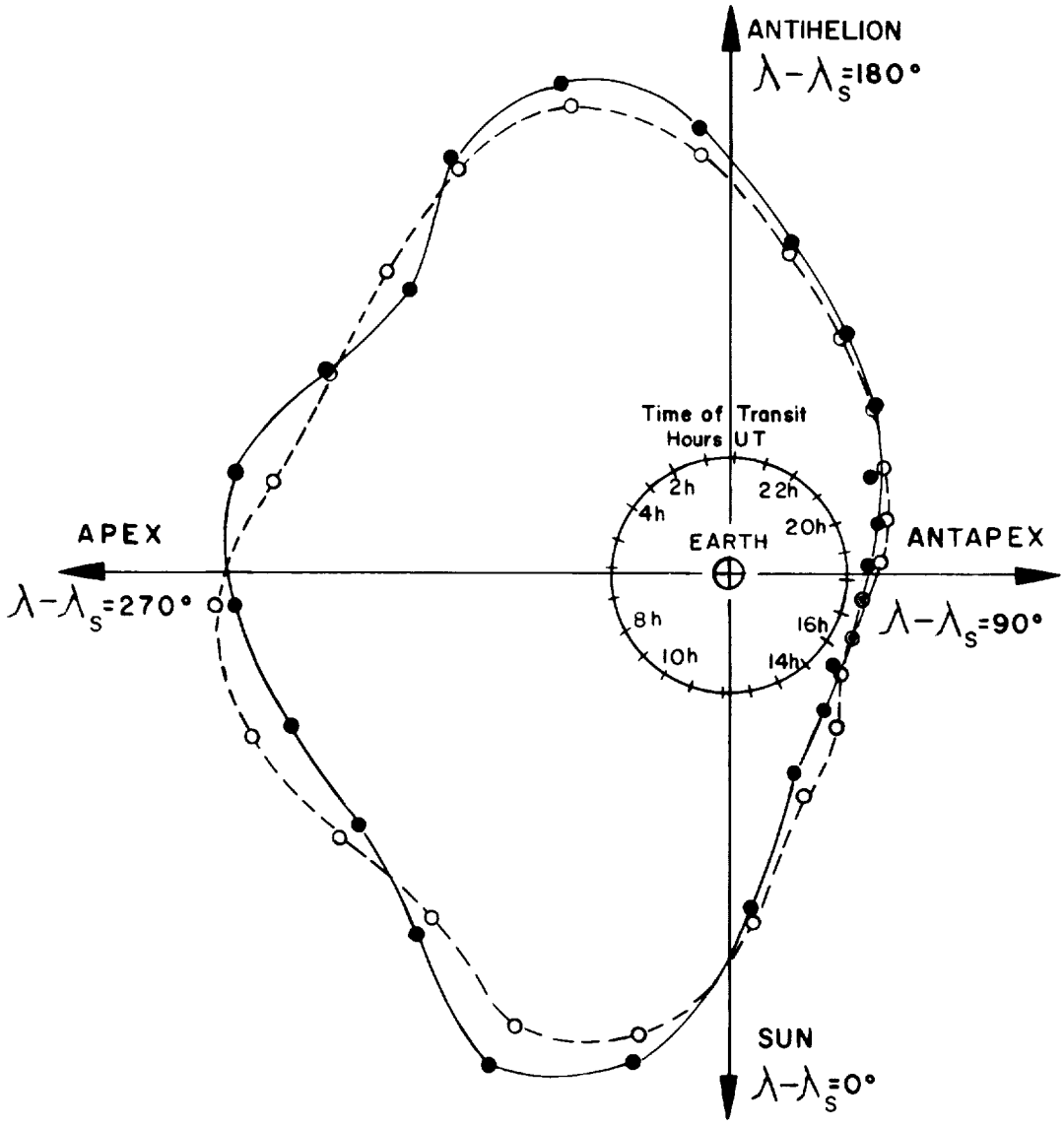

FIG. 15. POLAR DIAGRAM DRAWN IN THE PLANE OF THE EARTH'S ORBIT WHICH SHOWS THE APPARENT NUMBER OF METEOR RADIANTS DETECTED PER UNIT ANGLE, PER SECOND (REPRODUCTION OF FIGURE 7 OF REFERENCE 51)

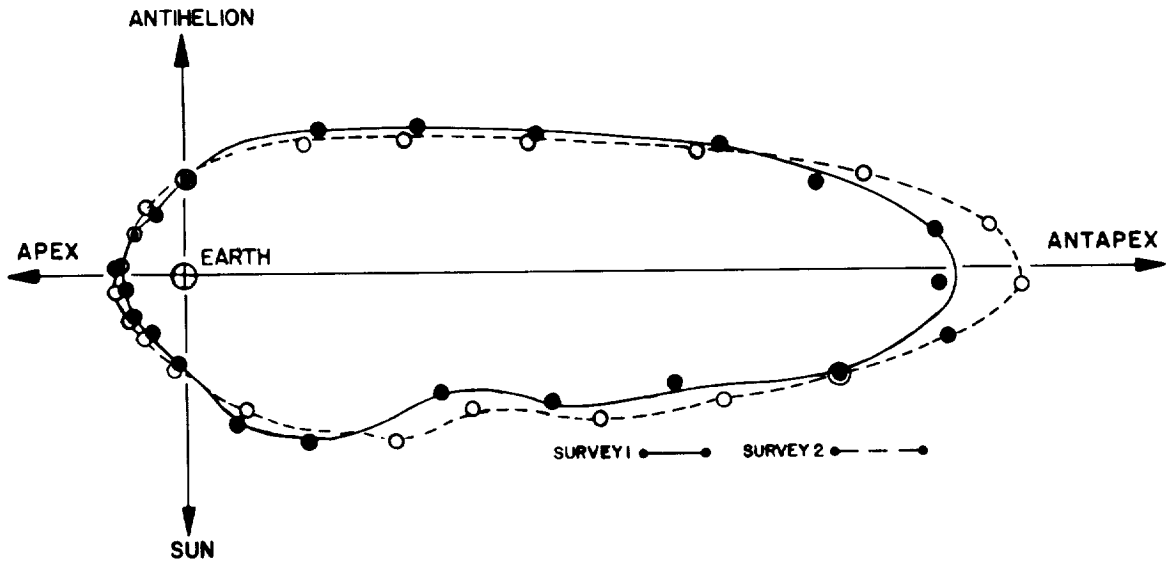

FIG. 16. POLAR DIAGRAM DRAWN IN THE PLANE OF THE EARTH'S ORBIT WHICH SHOWS THE NUMBER OF METEORS PER UNIT ANGLE WHICH CROSS THE EARTH'S ORBIT PER SECOND (REPRODUCTION OF FIGURE 8 OF REFERENCE 51)

REFERENCES

1. Alexander, W. M., McCracken, C. W., and LaGow, H. E. "Interplanetary Dust Particles of Micron-Size Probably Associated With the Leonid Meteor Stream," Journal of Geophysical Research, November 1961, Vol. 66, No. 11, pp. 3970-3973.

2. Baker, R. M., Jr., "Ephemeral Natural Satellites of the Earth," Science, 14 November 1958, Vol. 128, No. 3333, pp. 1211-1212.

3. Beard, D. B., "Interplanetary Dust Distribution and Erosion Effects," Surface Effects on Spacecraft Materials, 1st Symposium Ed., Clauss, F. J., 1960, pp. 378-390.

4. Bel'kovich, O. I., "A Determination of the Mean-Square Deviation of the Time-Rate of Meteors," Soviet Astronomy, Nov-Dec 1961, Vol. 5, No. 3, pp. 396-398.

5. Best, G. T., "The Accretion of Meteoritic Material by the Earth," Space Research, Proceedings of the First International Space Science Symposium, Ed., Bijl, H. K., Interscience Pub., 1960, pp. 1023-1032.

6. Bjork, R. L., "Meteoroids versus Space Vehicles," ARS Journal, June 1961, Vol. 31, No. 6, pp. 803-807.

7. Dalton, C. C., et.al., "Operational Effectiveness of HAWK and MARINE SPARROW Missile Systems," ORO-OML Report No. 5R2F, November 1955.

8. Dalton, C. C., "Propagation of Confidence Levels," ABMA Report No. DRR-TN-12-60, 11 May 1960.

9. Dalton, C. C., "Failure-Rate Assumptions and Calculation Methods," ABMA Report No. DRR-TN-14-60, 30 June 1960.

10. Dalton, C. C., "Confidence Levels and Standard Deviations for Successes versus Trials Ratios," MSFC Report No. M-REL-MTP-1-60, October 3, 1960.

REFERENCES (CONT.)

11. Dalton, C. C., "Mission Reliability of Boosted Flight for MERCURY-REDSTONE," MSFC Report No. MTP-M-RP-61-6, February 24, 1961.

12. Davison, E. H. and Winslow, P. C. Jr., "Space Debris Hazard Evaluation," NASA Technical Note D-1105, December 1961.

13. Davison, E. H., and Winslow, P.C. Jr., "Direct Evaluation of Meteoroid Hazard," Aerospace Engineering, February 1962, pp. 24-33.

14. Dubin, M., "IGY Micrometeorite Measurements," Space Research (see Ref. 5), pp. 1042-1058.

15. Dubin, M., "Meteoritic Dust Measured from Explorer I," Annals of the International Geophysical Year, Vol. XII, Part II, Pergamon Press, 1960, pp. 472-484.

16. Dubin, M., "Remarks on the Article by A. R. Hibbs, 'The Distribution of Micrometeorites Near the Earth,'" Journal of Geophysical Research, Vol. 66, No. 8, August 1961, pp. 2592-2594.

17. Eichelberger, R. J., and Gehring, J.W., "Effects of Meteoroid Impacts on Space Vehicles," American Rocket Society Paper No. 2030-61, Space Flight Report to the Nation, October 9-15, 1961.

18. Ellyett, C., and Keay, C.S.L., "All-Sky Meteor Rates in the Southern Hemisphere," Journal of Geophysical Research, Vol. 66, No. 8, August 1961, pp. 2590-2591.

19. Ehricke, K. A., "Space Flight, Vol. 1: Environment and Celestial Mechanics," Principles of Guided Missile Design, Ed., Merrill, G. M., D. van Nostrand Co., 1960.

20. Fisher, D. E., "Space Erosion of the Grant Meteorite," Journal of Geophysical Research, Vol. 66, No. 5, May 1961, pp. 1509-1511.

21. Friedman, H., "Physics of the Atmosphere and Space," Astronautics, Vol. 6, No. 12, December 1961, pp. 46, 92-94, 96.

22. Hibbs, A. R., "The Distribution of Micrometeorites Near the Earth," Journal of Geophysical Research, Vol. 66, No. 2, February 1961, pp. 371-377.

23. Hibbs, A. R., "Author's Reply to the Preceding Discussion on the Article, 'The Distribution of Micrometeorites Near the Earth,'" Journal of Geophysical Research, Vol. 66, No. 8, August 1961, pp. 2595-2596.

24. Hoel, P. G., "Introduction to Mathematical Statistics," John Wiley and Sons, Inc., 1947.

25. Hoenig, S. A., and Ritter, A.,"Problems in the Meteoric Erosion," Proceedings of the Second Hypervelocity and Impact Effects Symposium, Vol. 1, Ed., Mannix, W. C., et.al., December 1957, pp. 57-68.

26. Holl, H. B., "A Comparison of the Displacement of Satellites Caused by Meteoric Impacts and by Radiation Pressure," MSFC Report No. MTP-AERO-61-5, January 5, 1961.

27. Laevastu, T., and Mellis, O.,"Size and Mass Distribution of Cosmic Dust," Journal of Geophysical Research, Vol. 66, No. 8, August 1961, pp. 2507-2508.

28. LaGow, H. E., and Alexander, W. M.,"Recent Direct Measurements of Cosmic Dust in the Vicinity of the Earth Using Satellites," Space Research (see Ref. 5) pp. 1033-1041.

29. McCoy, T. M., "Hyperenvironment Simulation, Part 1: Definition and Effects of Space Vehicle Environment, Natural and Induced," Northrop Corp., Norair Div., Hawthorne, California, Report No. NOR60-289, September 1960, Contract No. AF 33(616)-6679, Project 0(1-1309); Task 13000.

30. McCracken, C. W., Alexander, W.M., and Dubin, M.,"Direct Measurements of Interplanetary Dust Particles in the Vicinity of the Earth," NASA Technical Note D-1174, December 1961.

31. Nazarova, T. N., "The Results of Studies of Meteoric Dust by Means of Sputnik III and Space Rockets," Space Research (see Ref. 5), pp. 1059-1062.

REFERENCES (CONT.)

32. Nazarova, T. N., "Investigation of Meteoric Particles by the Third Soviet Satellite," ARS Journal, Vol. 31, No. 9, September 1961, pp. 1341-1344.

33. Nysmith, C., and Summers, J. L., "Preliminary Investigation of Impact on Multiple-Sheet Structures and an Evaluation of the Meteoroid Hazard to Space Vehicles," NASA Technical Note D-1039, September 1961.

34. Rinehart, J. S., "Meteor Distribution and Cratering," Proceedings of the Second Hypervelocity and Impact Effects Symposium (see Ref. 25), pp. 45-53.

35. Rodriguez, D., "Meteoroid Shielding for Space Vehicles," Aerospace Engineering, December 1960, pp. 20-23, 55, 58, 60, 62, 64-66.

36. Scarborough, J. B., "Numerical Mathematical Analysis," Johns Hopkins Press, 1958.

37. Siedentopf, H., "Diffuse Matter in the Solar System," Meteors (A Symposium on Meteor Physics): Special Supplement (Vol. 2) to the Journal of Atmospheric and Terrestrial Physics, Ed., Kaiser, T. R., Pergamon Press, 1955, pp. 145-146.

38. Singer, F. S., "Reviewer's Comments" (on Ref. 32), ARS Journal, Vol. 31, No. 9, September 1961, p. 1344.

39. Toralballa, L. V., "Specific Mortality of Engineering Devices," Aero/Space Engineering, Vol. 18, No. 6, June 1959, pp. 41-42, 47.

40. Way, K., Gove, N. B., and van Lieshout, R., "Waiting for Mr. Know-It-All (or Scientific Information Tools We Could Have Now)," Physics Today, Vol. 15, No. 2, February 1962, pp. 22-24, 26-27.

41. Whipple, F. L., "The Meteoritic Risk to Space Vehicles," Vistas in Astronautics (First Annual Air Force Office of Scientific Research Astronautics Symposium), Ed., Alperin, M., and Sterm, M., Pergamon Press, 1958, pp. 115-124.

42. Whipple, F. L., "The Exploration of Space," Symposium on Space Physics, Ed. Jastrow, R., MacMillan Co., Reviewed by Koles, M. E., The Reflector, Vol. XII, No. 1, January-February-March 1962.

43. Öpik, E. J., Discussion at the end of the paper by Laevastu, T., and Mellis, O., "Extraterrestrial Material in Deep-Sea Deposits," Transactions, American Geophysical Union, Vol. 36, No. 3, June 1955, pp. 385-388.

44. Öpik, E. J., "The Masses and Structure of Meteors," Meteors (see Ref. 37).

45. Kallmann, H. K., "Relationship Between Masses and Visual Magnitudes of Meteors," Meteors (see Ref. 37).

46. Levin, B. J., "Physical Theory of Meteors and the Study of the Structure of the Complex of Meteor Bodies on the Basis of Visual Meteor Observations" (see Ref. 37).

47. Jacchia, L. G., "On Two Parameters Used in the Physical Theory of Meteors," Smithsonian Contributions to Astrophysics, Vol. 2, No. 9, 1958.

48. Herrmann, W., and Jones, A.H., "Survey of Hypervelocity Impact Information," Aeroelastic and Structures Research Laboratory, Massachusetts Institute of Technology, Report No. 99-1, September 1961.

49. Black, S. D., "Setting the Structural Design Criteria for Space Debris Effects in Cislunar and Outer Space Travel," Society of Automotive Engineers, National Aeronautic Meeting Report 520E, April 3-6, 1962.

50. "Metals Handbook," American Society of Metals, 1948.

51. Hawkins, G. S., "A Radio Survey of Sporadic Meteor Radiants," Royal Aeronautical Society, Monthly Notices, Vol. 116, No. 1, 1956, pp. 92-104.